Original Article

MOLECULAR METABOLISM

Predicting and understanding the response to short-term intensive insulin therapy in people with early type 2 diabetes

Yury O. Nunez Lopez [1], Ravi Retnakaran [2], Bernard Zinman [2], Richard E. Pratley [1,*], Attila A. Seyhan [1,3,4,]**

ABSTRACT

Objective: Short-term intensive insulin therapy (IIT) early in the course of type 2 diabetes acutely improves beta-cell function with long-lasting effects on glycemic control. However, conventional measures cannot determine which patients are better suited for IIT, and little is known about the molecular mechanisms determining response. Therefore, this study aimed to develop a model that could accurately predict the response to IIT and provide insight into molecular mechanisms driving such response in humans.

Methods: Twenty-four patients with early type 2 diabetes were assessed at baseline and four weeks after IIT, consisting of basal detemir and premeal insulin aspart. Twelve individuals had a beneficial beta-cell response to IIT (responders) and 12 did not (nonresponders). Beta-cell function was assessed by multiple methods, including Insulin Secretion-Sensitivity Index-2. MicroRNAs (miRNAs) were profiled in plasma samples before and after IIT. The response to IIT was modeled using a machine learning algorithm and potential miRNA-mediated regulatory mechanisms assessed by differential expression, correlation, and functional network analyses (FNA).

Results: Baseline levels of circulating miR-145-5p, miR-29c-3p, and HbA1c accurately (91.7%) predicted the response to IIT (OR = 121 [95% CI: 6.7, 2188.3]). Mechanistically, a previously described regulatory loop between miR-145-5p and miR-483-3p/5p, which controls TP53-mediated apoptosis, appears to also occur in our study population of humans with early type 2 diabetes. In addition, significant (fold change > 2, $P < 0.05$) longitudinal changes due to IIT in the circulating levels of miR-138-5p, miR-192-5p, miR-195-5p, miR-320b, and let-7a-5p further characterized the responder group and significantly correlated ($|r| > 0.4$, $P < 0.05$) with the changes in measures of beta-cell function and insulin sensitivity. FNA identified a network of coordinately/cooperatively regulated miRNA-targeted genes that potentially drives the IIT response through negative regulation of apoptotic processes that underlie beta cell dysfunction and concomitant positive regulation of proliferation.

Conclusions: Responses to IIT in people with early type 2 diabetes are associated with characteristic miRNA signatures. This study represents a first step to identify potential responders to IIT (a current limitation in the field) and provides important insight into the pathophysiologic determinants of the reversibility of beta-cell dysfunction.

ClinicalTrial.gov identifier: NCT01270789.

Keywords Short-term intensive insulin therapy; Beta-cell dysfunction; Type 2 diabetes; MicroRNA; Response prediction; Cooperative overtargeting

1. INTRODUCTION

Type 2 diabetes is characterized by multiple metabolic abnormalities including insulin resistance and beta-cell dysfunction which precede and predict the onset of the disease [1,2]. Metabolic function continues to deteriorate after diagnosis, leading to worsening hyperglycemia and necessitating insulin therapy in many cases. The progression of type 2 diabetes is thought to be due to a decline in pancreatic islet beta-cell function which can be explained by considering two components: 1) a "reversible" component due to the metabolic milieu (*e.g.* glucotoxicity, lipotoxicity), and 2) an "irreversible/intrinsic" component (*e.g.* loss of beta-cell capacity/mass due to beta-cell death), each independently contributing to the pathological process of the disease [3–5].

[1]Translational Research Institute for Metabolism and Diabetes, Florida Hospital, Orlando, FL 32804, USA [2]Lunenfeld-Tanenbaum Research Institute, Mount Sinai Hospital, Toronto, ON, Canada [3]The Chemical Engineering Department, Massachusetts Institute of Technology, Cambridge, MA, USA

[4] Current address: Fox Chase Cancer Center, Temple Health, Temple University, 333 Cottman Avenue, Philadelphia, PA, USA. Fax: +1 215 214 1590.

*Corresponding author. Translational Research Institute for Metabolism and Diabetes, Florida Hospital Translational Research Institute, 301 East Princeton Street, Orlando, FL 32804, USA. Fax: +1 407 303 7199. E-mail: Richard.Pratley@flhosp.org (R.E. Pratley).

**Corresponding author. Translational Research Institute for Metabolism and Diabetes, Florida Hospital Translational Research Institute, 301 East Princeton Street, Orlando, FL 32804, USA. Fax: +1 407 303 7199. E-mail: Attila.Seyhan@fccc.edu (A.A. Seyhan).

Received September 10, 2018 • Revision received November 5, 2018 • Accepted November 12, 2018 • Available online 16 November 2018

https://doi.org/10.1016/j.molmet.2018.11.003

Short-term (two to four week) intensive insulin therapy (IIT) administered early in the course of type 2 diabetes acutely improves beta-cell function by eliminating glucotoxicity and lipotoxicity [6–9]. Remarkably, this strategy can induce "glycemic remission" in some patients who can subsequently maintain normoglycemia without antidiabetic drugs for up to 1–2 years [10]. However, this beneficial effect is not seen in all patients [11]. Similarly, short-term IIT is also effective in patients with established type 2 diabetes of longer duration, albeit with more variability in the response [12]. This heterogeneity in the response to short-term IIT may reflect varying contributions of reversible and irreversible beta-cell dysfunction, components that cannot be determined using clinical parameters or conventional measures of beta-cell function. Thus, the identification of biomarkers that can predict the response to short-term IIT and other therapeutic interventions would be valuable for improving treatment decisions and outcomes. Such biomarkers might also provide insight into novel molecular mechanisms involved in disease pathogenesis.

MicroRNAs (miRNAs) are endogenous, noncoding RNAs that are abundantly expressed in most cell types and tissues and play important roles in the regulation of a broad spectrum of physiological and pathological processes, including diabetes [13–16]. Altered miRNA levels in the circulation have been associated with a variety of disease states including obesity [17–21] and diabetes [22–27]. We hypothesized that circulating levels of miRNAs implicated in beta-cell dysfunction and insulin resistance (*e.g.*, involving adipose tissue, liver, skeletal muscle) might be useful to predict responses to therapies such as short-term IIT. To test this hypothesis, we assessed changes in a panel of miRNAs implicated in diabetes in response to short-term IIT in patients with early type 2 diabetes and explored potential mechanisms underlying the reversibility of beta-cell dysfunction. This study is the first assessing the miRNA response to short-term IIT and offers novel mechanistic insights into the pathophysiology of beta-cell dysfunction in early type 2 diabetes.

2. METHODS

2.1. Study population

The study population consisted of 24 adult patients with early type 2 diabetes who underwent short-term IIT to determine eligibility for randomization in the **LI**raglutide and **B**eta-cell **R**ep**A**ir (LIBRA) Trial (clinicaltrial.gov identifier: NCT01270789) [4,11,28]. The LIBRA trial included participants with 1) duration of diabetes $\leq$7 years, 2) treatment with none or up to two oral antidiabetic medications (which were stopped before starting IIT), and 3) hemoglobin HbA1c at screening between 5.5 and 9.0% inclusive if on oral antidiabetic medications or between 6.0 and 10.0% inclusive if not on antidiabetic medications. Exclusion criteria included insulin therapy, renal dysfunction, hepatic dysfunction, malignancy and chronic infection. The study protocol was approved by the Mount Sinai Hospital Research Ethics Board, and all participants provided written informed consent.

2.2. Study design

In the LIBRA trial [28], 63 participants underwent 4-weeks of intensive insulin therapy (IIT). On the final day of IIT, the last insulin dose was the bolus insulin before dinner, with no bedtime basal insulin. To be eligible for randomization, participants needed to be able to maintain fasting venous glucose $<$7.0 mmol/l the next morning, reflecting the capacity of endogenous insulin secretion to maintain fasting glucose in the non-diabetic range. The achievement of this threshold was previously shown to identify reversibility of beta-cell dysfunction in response to IIT [12]. Of the 63 LIBRA participants, there were 12 individuals who did not achieve this threshold and hence were not eligible for randomization. These 12 individuals comprised the nonresponder (NR) group for the current study (this study). Conversely, the responder (R) group was comprised of the 12 LIBRA participants who had the largest improvement in beta-cell function from baseline to the post-IIT assessment (as defined by the percentage increase in Insulin Secretion-Sensitivity Index-2 (ISSI-2)). While there was no prospective measure of efficacy of IIT in the current analysis, it should be recognized that the beneficial effect of IIT on beta-cell function in early type 2 diabetes has been well-established in previous studies, including a meta-analysis of the studies comprising this literature [10]. In the current study, all participants thus underwent assessment of beta-cell function before and after IIT, which enabled systematic assessment of the impact of IIT on beta-cell function and stratification of participants into responders and nonresponders on this basis.

The specific short-term IIT protocol, methods for laboratory measurements, and calculation of physiologic indices performed in this trial are described elsewhere [4,11,28]. Glucagon measurements were performed using a glucagon enzyme-linked immunosorbent assay 10-1271-01 from Mercodia (Uppsala, Sweden) as recently described [29]. Beta-cell function was measured with the ISSI-2 index, which was the primary outcome measure in the LIBRA Trial [28]. In addition, other indices of beta-cell function and insulin resistance were calculated from the OGTT, including the $\Delta ISR_{0\text{-}120}/\Delta Gluc_{0\text{-}120} \times$ Matsuda index and the homeostatic model assessment of insulin resistance (HOMA-IR) [4,11,28]. miRNA was isolated from the fasting baseline pre-IIT OGTT and post-IIT OGTT plasma samples. A custom panel of 94 miRNAs (Supplementary Table ST1) reported to play roles in metabolically-involved tissues such as adipose, brain, kidney, liver, muscle, and pancreas was measured by real-time PCR. All baseline clinical and biochemical data was used to generate a classifier with predictive value by implementing a machine learning approach based on the random forest algorithm [30] (see Methods section: Predictive modeling). To gain additional biological insight of the mechanism of response to short-term IIT, we conducted differential miRNA expression analysis by implementing mixed-effect models for repeated measures (see Methods section: Statistical analysis) and miRNA–mRNA interaction network analysis (as described in the Methods section: Functional network analysis).

2.3. Measurement of plasma miRNAs

miRNAs from 200 µl plasma were extracted using the miRNeasy Serum/Plasma Kit (Qiagen, Hilden, Germany), reverse transcribed, preamplified, and measured by quantitative real-time PCR using TaqMan® reagents and ViiA-7® instrument from ThermoFisher Scientific (Waltham, MA), following the manufacturer's instructions. Custom TaqMan® Array MicroRNA Cards from a single production batch were used. Data was analyzed using the *HTqPCR* package in the R 3.5.1 statistical computing environment [31]. Data from each sample were first normalized to the levels of recovered spike-in cel-miR-39, then subjected to quantile normalization using the *normalizeCtData* function. The median of the quantile-normalized data for the NR group, pre-IIT time point, was then subtracted from each quantile-normalized value to generate $-\Delta\Delta$Ct data equivalent to log2 fold change data (denoted herein logFC). As hemolysis during plasma isolation could contaminate the specific pool of circulating miRNAs and contribute to degradation of sample quality [32], its impact was assessed by calculating the difference in logFC values between erythrocyte-enriched miR-451 and reference miR-23a-3p (hemolysis score $=$ $\text{logFC}_{\text{miR-451}} - \text{logFC}_{\text{miR-23a-3p}}$; equivalent to the log2 ratio between miR-451 and miR-23a-3p), which can detect very low levels of hemolysis [33,34]. A hemolysis score lower than 7 was required by study design for samples to be included in the final analysis.

Only miRNAs with greater than 2-fold baseline-adjusted differences between R and NR groups were included in the reported differential abundance analysis.

2.4. Predictive modeling

To the limitations of a small sample size, we selected a machine learning approach based on the random forests (RF) method, which implements an out-of-bag ("bagging") technique to monitor error and ensure unbiased prediction with reduced risk of overfitting [30]. As reported by [30], "by using bagging in tandem with random feature selection, the out-of-bag error estimate is as accurate as using a test set of the same size as the training set. Therefore, using the out-of-bag error estimate removes the need for a set aside test set." [30] In short: each new training set is drawn, with replacement, from the original training set (with each bootstrapped training set leaving about one-third of the instances out — the out-of-bag (OOB) set); then a tree is grown on the new training set using random feature selection. Furthermore, because the RF variable selection process uses only a small random subset of predictor variables for each tree split in the classification tree, the technique can handle the "small *n* large *p*" problem, where the number of predictor variables (*p*) is greater than the number of subjects (*n*) [35]. Regarding the diagnosis of human disorders, it has been demonstrated that, by means of the repeated random sampling from the learning data, RF automatically generates realistic estimates of the prediction accuracy on validation data [35,36].

For our analysis, the RF algorithm was implemented using the *randomForest* package [37] in the R environment. Only baseline values for all profiled miRNAs and clinical and metabolic measures were included as variables for tree splitting and classification. A twofold-iterative process of repeated, sequential backward elimination (SBE) [38] was implemented. Each repetition of SBE (the "inner loop") consisted of successive cycles of RF classification whereby the less informative variable (as calculated by the Gini variable importance index) was eliminated after every cycle, until a single variable remained in the classifier. The number of trees (*ntree*) in the forest was always set to 5000 and the number of variables to be randomly sampled at each tree split (*mtry*) set equal to the total number of variables included in the given SBE "inner cycle". The OOB prediction error rate calculated for each instance of the RF classifier was recorded and the instance(s) generating the lower error rate selected as the optimal RF classifier(s) for the given SBE repetition. The SBE process was repeated 100 times (the "outer loop"), while choosing a distinct random number generator seed for each "outer cycle". The collection of optimal RF classifiers with minimal OOB error rates for all 100 repetitions of the SBE process was then summarized and the most frequent instance of the RF classifier consistently producing the lowest OOB error rate was identified. Performance and sensitivity analysis of the best classifier was evaluated and visualized using the *ROCR* package in the R environment. ROC curves were generated by using the random forest responder/nonresponder vote fractions (based on the OOB data) as prediction scores to construct the ROC curves by stepping through different thresholds for calling responder versus nonresponder. By comparing these predictions based on the out-of-bag data to their known class, estimates of the performance of the classifier can be obtained.

2.5. Functional network analysis (FNA)

Our previous experience and that from others studying disparate molecular mechanisms regulated by miRNAs indicate that global biologically significant miRNA-driven regulatory events commonly occur in a coordinated/cooperative fashion [39—46]. This process can be readily described by a compact network of interactions between relevant miRNAs and corresponding "miRNA-overtargeted" genes [40,42—45]. The "overtargeted" genes in a particular network appear to interact with a significantly higher number of miRNAs than expected by chance (as determined by hypergeometric tests of network proportions compared to the respective proportions in the miRNA—target interaction universe/background). In this study, we similarly conducted miRNA-overtargeting analyses following our published methodology [40,42,44,45]. Significance of the cooperative (more than 1 miRNA targeting a given gene) and overtargeting effect (significant higher number of miRNA-targeting events than expected by chance on a given gene) was assessed by comparing IIT-specific network proportions and relevant number of events against a collection of 10,000 simulated equivalent random networks. The list of validated targets supported by strong experimental evidence (*i.e.*, reporter assay or Western blot) used for this analysis was downloaded from miRTarBase (file: miRTarBase_SE_WR.xls) using the *SpidermiR* package [47]. Interaction networks were constructed using Cytoscape 3.5.1 [48]. Enrichment of gene ontology annotations among sets of overtargeted genes was assessed using the *GOCluster_Report* function of the *systemPipeR* package [49] in the R environment.

2.6. Statistical analysis

Data normality was tested with the Shapiro—Wilk test. Data were log or square root transformed to approximate normality when necessary. Differences in baseline clinical characteristics were assessed using the Welch two sample t test (for continuous variables) or the Fisher exact test (for categorical variables). Standard Pearson's correlations between baseline levels of clinical/metabolic variables and the percent change in ISSI-2 were calculated to identify potential confounding covariates. For assessment of longitudinal differences in clinical, metabolic, and circulating miRNA variables, mixed-effect models for repeated measures were implemented using the *lme4* package. Age, duration of diabetes, baseline HbA1c, baseline AUC glucagon, and baseline HOMA-IR measures were included in the model as covariates to adjust for potential confounding effects, given their relevant correlations with the percent change in ISSI-2 (absolute $|r| > 0.4$, $P < 0.05$). Post-hoc analysis was performed using the *phia* package. Partial correlations adjusting for the same covariates, were calculated using the *ppcor* package. Calculated effects and partial correlations were considered significant at $P < 0.05$. False discovery rates (FDR) correcting for multiple testing were calculated using the Benjamini-Hochberg correction. Principal component analysis (PCA) using functions from the *HTqPCR* packages was used for high dimensional assessment and visualization of miRNA expression changes.

2.7. Power calculation

Based on our data using equivalent miRNA profiling technology, we previously determined that a minimum sample size of $N = 11$ subjects per group will detect a 1.5-fold change in the levels of circulating miRNAs with 80% power at a two-sided significance level $\alpha = 0.05$ [50,51]. This study, with a slightly larger sample size ($N = 12$ per group) and a larger effect size required as per study design (miRNA fold change between groups greater than two), was designed to detect significant differences with greater than 80% statistical power.

3. RESULTS

3.1. Study participants

Table 1 shows the baseline characteristics of the study cohort and highlights baseline group differences and correlations to the

primary outcome variable, namely percent change in ISSI-2. These baseline imbalances (in duration of diabetes, HbA1c, HOMA-IR and AUC glucagon, $P < 0.05$) and most notably, the existence of significant correlations (absolute $|r| > 0.4$, $P < 0.05$) between the percent change in ISSI-2 and the baseline levels of HbA1c, AUC glucagon, and age, respectively, identified these variables as potential confounders that needed to be adjusted for during statistical modeling.

3.2. Improvements in beta-cell function and insulin sensitivity in response to short-term IIT

As reported in the parent trial [28] and by selection in the current secondary analysis, people in the R group experienced a dramatic increase in ISSI-2 (greater than 2-fold increase), whereas people in the NR group displayed a nonsignificant reduction (Group-by-Time interaction effect FDR < 0.001, Supplementary Table ST2), even after adjusting for confounding effects of age, duration of diabetes, and baseline levels of HbA1c, HOMA-IR, and AUC glucagon. Notably, insulin resistance (as measured by the HOMA-IR index) significantly improved in the R group only (Group-by-Time interaction effect FDR < 0.01, Supplementary Table ST2). In addition, people that responded to short-term IIT significantly reduced their fasting glucose and insulin levels and were able to significantly reduce their levels of glycated hemoglobin HbA1c by close to a full percent unit on average, as compared to the respective baseline levels (all three comparisons displaying Group-by-Time interaction effects with $P \leq 0.0268$ and FDR ≤ 0.0603, Supplementary Table ST2). Although to a lesser extent, short-term IIT also reduced HbA1c levels in the NR group resulting in a significant Time effect for this measure ($P = 0.001$, FDR < 0.01).

Table 1 — Baseline characteristics of the study cohort.

A. Baseline characteristics	Level	Nonresponder (n = 12)	Responder (n = 12)	*P* value
Gender (%)	Female	4 (33.3)	3 (25.0)	1
	Male	8 (66.7)	9 (75.0)	
Ethnicity (%)	Other	2 (16.7)	2 (16.7)	1
	White	10 (83.3)	10 (83.3)	
Age (years)		62.8 (8.3)	56.0 (10.2)	0.085
Duration of diabetes (years)[†]		4.5 (2.3)	2.3 (2.4)	0.026
Pre-study metformin (%)	0	2 (16.7)	5 (41.7)	0.369
	1	10 (83.3)	7 (58.3)	
Pre-study sulfonylurea (%)	0	10 (83.3)	11 (91.7)	1
	1	2 (16.7)	1 (8.3)	
Pre-study oral agents (%)	0	2 (16.7)	5 (41.7)	0.369
	1	10 (83.3)	7 (58.3)	
BMI (kg/m^2)		28.7 (4.6)	30.7 (4.1)	0.283
Waist circumference(cm)		97.9 (10.2)	105.5 (11.8)	0.104
HbA1c (%)[§]		6.7 (0.4)	7.6 (1.2)	0.022
Fasting glucose (mmol/L)		7.6 (1.1)	7.5 (1.6)	0.883
Fasting insulin (mmol/L)[§]		91.9 (59.6)	159.7 (149.5)	0.058
Fasting glucagon (Mercodia) (mmol/L)		6.2 (2.3)	7.9 (3.5)	0.169
AUC glucagon (Mercodia)		19.3 (4.6)	27.5 (9.5)	0.013
2-hour glucose on OGTT (mmol/L)		17.3 (2.5)	16.1 (4.0)	0.391
HOMA IR[§]		4.5 (3.1)	7.5 (6.5)	0.086
ISSI-2		113.0 (31.4)	135.0 (62.7)	0.289
ISR0-120/Gluc0-120×Matsuda index		0.10 (0.04)	0.09 (0.07)	0.698
B. Standard baseline correlations to % change in ISSI-2		**n**	**cor**	***P* value**
HbA1c[§]		24	0.69	2.1E-04
AUC glucagon (Mercodia)		24	0.54	0.007
Age		24	−0.44	0.032
Duration of diabetes[†]		24	−0.44	0.033
HOMA IR[§]		24	0.42	0.044
Waist circumference		24	0.36	0.081
Fasting insulin[§]		24	0.36	0.082
Fasting glucagon (Mercodia)		24	0.35	0.093
Fasting glucose		24	0.31	0.141
BMI		24	0.29	0.171
ISR0-120/Gluc0-120×Matsuda		24	−0.29	0.173
2-hour glucose		24	0.13	0.537
ISSI-2		24	−0.12	0.572

Data sqrt(†) or log(§) transformed to approximate normality for statistical inference tests.
Unadjusted differences in baseline measures were determined using the Welch two sample t test (for continuous variables) or the Fisher exact test (for categorical variables). Data is presented as mean with standard deviation or as percentage (%). Standard Pearson's correlation between baseline levels of clinical/metabolic variables and the percent change in ISSI-2 were calculated to identify potential confounding covariates.

3.3. MiRNA-based score of plasma quality

The quality of the initial plasma samples was assessed by calculating a hemolysis score per sample, as described in Material and Methods. All samples produced hemolysis scores below five (Supplementary Figure SF1). Therefore, following reported guidance [33,34], the risk of contamination by hemolysis was considered insignificant.

3.4. Baseline abundance of miR-145-5p, miR-29c-3p, together with baseline measures of glycated hemoglobin HbA1c accurately predict response to short-term IIT

To assess the potential of circulating miRNAs and clinical/metabolic measures to predict, at baseline, responses to short-term IIT, we implemented a comprehensive classification approach based on an RF algorithm using the *randomForest* package in the R environment. By implementing 100 iterations of an SBE approach, 159 optimal classifiers with minimal cross-validated error rate (OOB error rate = 8.3%) were generated. Baseline measurements of the trio miR-145-5p, miR-29c-3p, and HbA1c produced the best classifier 100 percent of the time, while the simpler classifier containing miR-145-5p and miR-29c-3p also attained the lowest error rate but only 56 percent of the time. A third more complex classifier including the above-mentioned trio and miR-326 also attained the lowest error rate but with a 2 percent frequency only. No combination of clinical parameters only (excluding miRNAs) generated an optimal classifier. Therefore, the RF classifier based on baseline measures of miR-145-5p, miR-29c-3p, and HbA1c was selected as the best RF classifier of response to short-term IIT. Figure 1 and Supplementary Figure SF2 show the longitudinal data for the three features comprising the best classifier and a variety of performance measures demonstrating the high sensitivity (area under the receiver operator characteristic AUC = 0.951) and accuracy (positive and negative predictive values both equal to 91.7%) of the classifier. Although the baseline-adjusted changes in miR-145-5p and miR-29c-3p in response to short-term IIT were not significantly different between the two groups as per our study criteria (Table 2), there was a trend (Group-by-Time interaction $P = 0.0547$) for miR-145-5p to differentially increase with time in the responder group. However, the median post-therapy miR-145-5p level in this group was still lower than the nonresponder level (Figure 1A). Importantly, the baseline levels of plasma miR-145-5p significantly correlated with the percent change in ISSI-2 ($r = -0.66$, $P = 0.0005$; Figure 1D upper panel), the change in HbA1c ($r = 0.48$, $P = 0.0164$; Figure 1E, upper panel), and with the change in fasting glucose levels ($r = 0.51$, $P = 0.0101$; Figure 1F, upper panel). These correlations support the identification of miR-145-5p as a key variable in the RF classifier

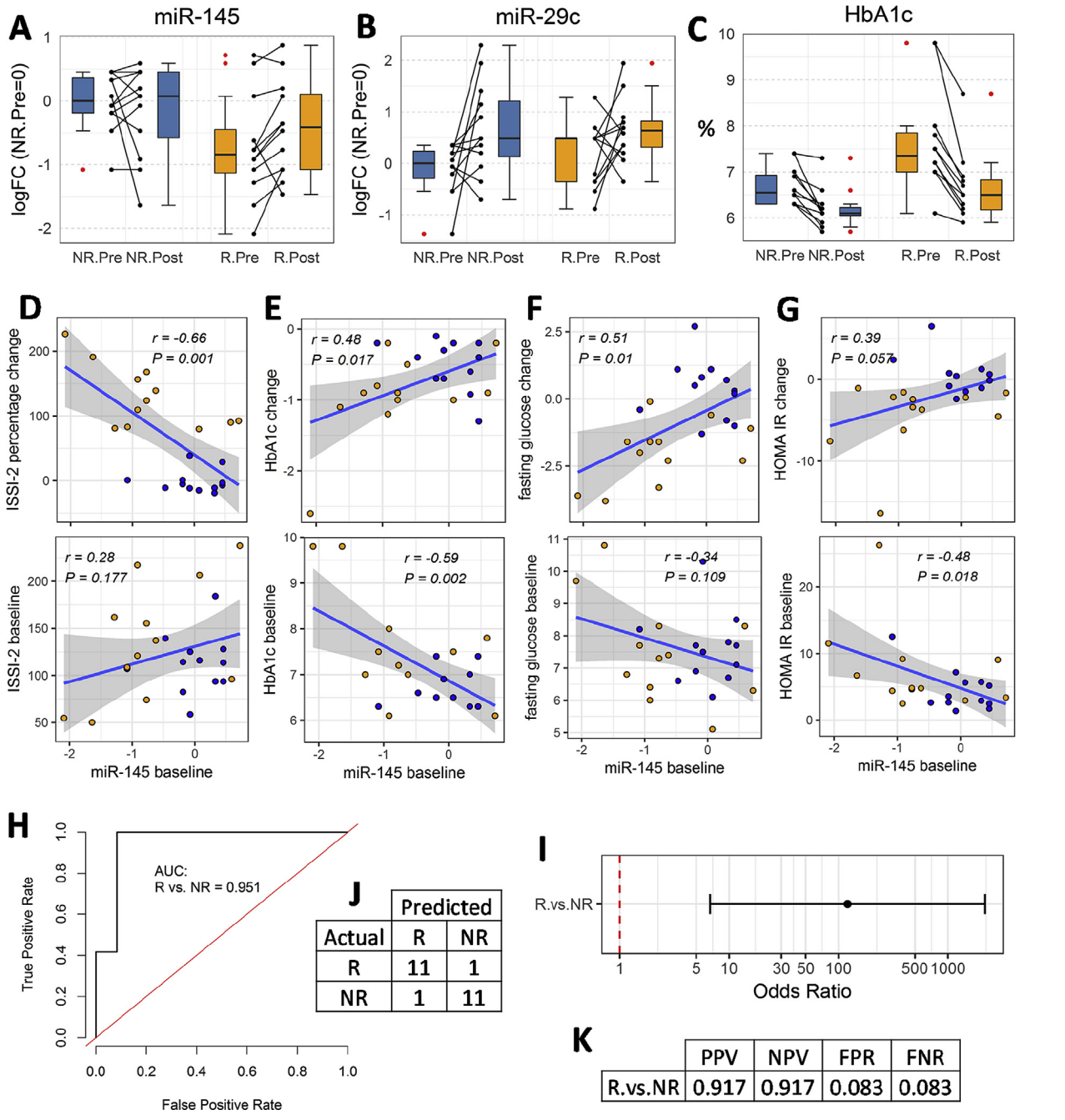

Figure 1: Identification of an optimal miRNA classifier for response to short-term IIT and summary of performance measures following an iterative random forests (RF) approach. (**A**–**C**) Dual plots for features comprising the best classifier of response. (**D**–**G**) Correlations between baseline levels of miR-145-5p and changes in measures of beta cell function and glucose control. ISSI-2 was the main outcome measure of beta-cell function, in the parent LIBRA trial, in response to short-term IIT. (**H**) Sensitivity analysis using the receiver operator characteristic curve (ROC). (**I**) Odds ratio plot for the classification using the best RF classifier. (**J**) Confusion matrix for the best RF classifier. (**K**) Performance measures for the best RF classifier. Orange-filled circles represent individual values for Responder (R) group. Blue-filled circles represent individual values for Nonresponder (NR) group. AUC: area under the ROC curve; PPV: positive predictive value; NPV: negative predictive value; FPR: false positive rate; FNR: false negative rate.

predictive of short-term IIT response and indicate that the lower the baseline levels of circulating miR-145-5p, the larger the subsequent short-term IIT-driven improvement in beta-cell function (as estimated by ISSI-2), reduction in HbA1c levels, and reduction in fasting glucose levels. Additionally, baseline levels of miR-145-5p significantly correlated with baseline levels of HbA1c ($r = -0.59$, $P = 0.0024$; Figure 1E, lower panel) and insulin resistance, as indicated by the HOMA-IR index ($r = -0.48$, $P = 0.0183$; Figure 1G, lower panel).

3.5. Validation of a potential regulatory association between miR-145-5p and miR-483-5p/3p

While revising the recent literature for the predictive miRNAs, we uncovered a potential mechanistically-relevant link between IIT response-predictive miR-145-5p and miR-483-5p/3p (the sense and corresponding antisense miRNAs originating from the same primary miR-483). The latter miRNAs were not originally included in our panel. Specifically, miR-145-5p and miR-483-3p are reported to be involved

Table 2 — Several miRNAs are differential abundant in the circulation of participants in responders and nonresponders.

	Nonresponders (NR) (n = 12)		Responders (R) (n = 12)		*P* values			FDR values		
	Pre	Post	Pre	Post	Group	Time	Group-by-Time	Group	Time	Group-by-Time
Pattern A										
miR.192	0.0 (−3.2, 3.5)	0.9 (−1.2, 3.2)	2.0 (−1.5, 3.3)	−1.6 (−5.7, 1.9)	0.0759	0.5175	**0.0004**	0.4089	0.6116	**0.0104**
miR.320b	0.0 (−0.8, 2.0)	0.2 (−0.8, 2.7)	0.7 (−0.4, 1.6)	−0.1 (−1.6, 1.0)	0.1489	0.4613	**0.0325**	0.4839	0.5825	**0.2028**
miR.195	0.0 (−2.3, 1.4)	0.7 (−0.1, 2.4)	0.3 (−0.1, 1.7)	0.4 (−0.5, 2.5)	0.1101	0.0018	**0.0364**	0.4089	0.0156	**0.2028**
let.7a	0.0 (−1.7, 0.5)	−0.4 (−3.5, 0.5)	−0.7 (−1.5, 0.9)	−0.2 (−1.1, 0.9)	0.7438	0.0562	**0.0384**	0.9205	0.1624	**0.2028**
miR.138	0.0 (−3.2, 7.8)	−3.0 (−3.6, 6.5)	−0.9 (−3.6, 6.5)	4.4 (−3.5, 7.1)	0.7129	0.1627	**0.0390**	0.9205	0.3525	**0.2028**
Pattern B										
miR.20a	0.0 (−0.5, 1.7)	1.3 (0.9, 2.6)	0.3 (−0.3, 2.6)	1.5 (−0.1, 2.6)	0.2863	**0.0001**	0.3905	0.6203	**0.0026**	0.7529
let.7b	0.0 (−1.1, 0.3)	0.6 (−0.1, 1.9)	−0.1 (−0.8, 0.8)	0.9 (0.6, 2.2)	0.3767	**0.0002**	0.6532	0.7534	**0.0026**	0.7949
miR.802	0.0 (−3.6, 4.2)	−3.3 (−5.1, 2.8)	−1.0 (−3.6, 2.2)	−4.1 (−5.0, 6.1)	0.4783	**0.0031**	0.3959	0.8291	**0.0201**	0.7529
miR.34a	0.0 (−3.4, 2.2)	−1.1 (−4.3, 1.9)	−0.5 (−2.0, 1.7)	−1.3 (−3.6, 0.7)	0.8851	**0.005**	0.7357	0.9205	**0.026**	0.8317
miR.144	0.0 (−6.1, 3.9)	3.1 (−1.9, 4.7)	−0.5 (−6.8, 4.1)	2.4 (−2.1, 3.9)	0.8685	**0.0117**	0.9194	0.9205	**0.0507**	0.9562
miR.183	0.0 (−7.5, 1.6)	1.7 (−6.7, 4.0)	0.9 (−2.9, 3.0)	1.2 (−2.9, 3.5)	0.0725	**0.0191**	0.1832	0.4089	**0.0709**	0.5954
miR.15b	0.0 (−0.4, 2.0)	−0.6 (−2.9, 0.7)	−0.2 (−3.1, 0.7)	−0.9 (−4.2, 2.9)	0.7236	**0.0331**	0.4054	0.9205	**0.1076**	0.7529
Predictive										
miR.145	0.0 (−0.9, 0.5)	0.1 (−1.5, 0.6)	−0.8 (−2.0, 0.7)	−0.4 (−1.4, 0.8)	0.2702	0.3457	0.0547	0.5404	0.3457	0.1094
miR.29c	0.0 (−1.1, 0.4)	0.5 (−0.6, 2.2)	0.5 (−0.8, 1.1)	0.6 (−0.2, 1.8)	0.5649	0.0057	0.4415	0.5649	0.0114	0.4415
Correlative										
miR.483.5p	0.0 (−1.1, 0.7)	−0.6 (−2.1, 0.2)	0.6 (−1.2, 1.9)	−0.6 (−1.8, 0.4)	0.2423	0.0041	0.1376	0.8211	0.0178	0.4763
miR.483.3p	0.0 (−1.5, 1.4)	−1.0 (−4.1, 0.7)	0.2 (−1.0, 1.6)	−0.5 (−2.4, 0.2)	0.713	0.0018	0.6664	0.9209	0.0116	0.7726

Pattern A miRNAs are characterized by significant Group-by-Time interaction effects (Fold Change > 2, $P < 0.05$ and FDR ≤ 0.2028), generally due to changes either in only one of the groups or in opposite directions in both R and NR groups. Pattern B miRNAs are characterized by significant Time effect (Fold Change > 2, $P < 0.05$ and FDR < 0.1), generally due to either a significant reduction or significant increase in plasma levels in both R and NR groups. Predictive miRNAs (as part of an RF classifier), although not considered differentially expressed by the study design criteria, are able to predict response to short-term IIT at baseline (pre-treatment stage). Both strands of miR-483 (-5p/-3p, potentially involved in regulatory loop with miR-145-5p) are stably detected and highly correlated among themselves and with miR-145-5p and miR-29c, respectively. Data is presented as median log2 fold change [relative to the median of the NR group baseline (Pre-IIT time point)], with 95% confidence interval in parenthesis. FDR calculated using the Benjamini-Hochberg correction.

in a glucose level-dependent loop that regulates miR-145-induced TP53-dependent cell death in hepatocellular carcinoma [52]. On the other hand, the complementary strand miR-483-5p has been reported to be differentially expressed in pancreatic α and β cells, and to protect against proinflammatory cytokine-induced apoptosis of β cells in culture and in mice, while increasing insulin transcription and secretion by the β cells and reducing glucagon transcription and secretion by the α cells [53]. Therefore, we hypothesized that the miR-145/miR-483 regulatory loop may play a mechanistic role contributing to the response to short-term IIT in humans. To assess the potential association between miR-145-5p and miR-483 in humans with diabetes, we then profiled both miR-483-3p and miR-483-5p in this study's plasma samples using TaqMan® assays and quantitative real time PCR (these measurements were normalized against the expression of the internal/endogenous control miR-191, Figure 2A, D). Supporting our hypothesis, we found that circulating levels of miR-483-5p significantly negatively correlated with circulating levels of miR-145-5p ($r = -0.34$, $P = 0.0203$, Figure 2B) and positively with miR-192-5p (an IIT-responsive miRNA reported in the next section, $r = 0.38$, $P = 0.009$, Figure 2C). Remarkably, the baseline circulating levels of miR-483-5p significantly correlated (absolute $|r| > 0.3$ and $P < 0.05$) with the baseline levels and the change in levels of HbA1c, fasting insulin, HOMA IR, AUC of the response to glucagon (Figure 2H—G), as well as with the change in fasting glucose levels (Figure 2L). On the other hand, levels of miR-483-5p expectedly and highly significantly correlated with the levels of miR-483-3p ($r = 0.53$, $P = 1.30 \times 10^{-04}$, Figure 2E), and the levels of miR-483-3p highly significantly negatively correlated with the levels of miR-29c-3p, the other IIT response-predictive miRNA ($r = -0.58$, $P = 2.32 \times 10^{-05}$, Figure 2F) and with miR-195-5p (an IIT-responsive miRNA reported in the next section, $r = -0.47$, $P = 0.001$, Figure 2G). Despite these strong correlations with clinical changes relevant to the response to short-term IIT, when baseline normalized miR-483 data was included among the set of baseline variables used to generate the RF classifiers and the BSE iterative RF process repeated, the optimal RF classifier continued to be comprised of the same three variables, namely miR-145-5p, miR-29c-3p, and HbA1c.

3.6. Circulating levels of miR-138-5p, miR-192-5p, miR-195-5p, miR-320b, and let-7a-5p differentially change in response to short-term IIT

To gain insight into potential miRNA-regulated mechanisms in response to short-term IIT, we evaluated the baseline and four-week follow-up changes in circulating miRNA levels and assessed the correlations between these changes and the changes in clinically relevant measures of beta-cell function (*i.e.*, ISSI-2 and $\Delta ISR_{0\text{-}120}/\Delta Gluc_{0\text{-}120} \times$Matsuda index), insulin resistance (*i.e.*, HOMA-IR), glycemic control (*e.g.*, HbA1c), and glucagon response (*e.g.*, AUC glucagon). We anticipated that changes in short-term IIT-responsive miRNAs would track with improvements in beta-cell function and insulin sensitivity, among others. As shown in Table 2, five circulating miRNAs (Pattern A: miR-138-5p, miR-192-5p, miR195-5p, miR-320b, and let-7a-5p) displayed significant differential expression changes (as denoted by the significant Group-by-Time interactions ($P < 0.05$ and FDR ≤ 0.2)) in response to short-term-IIT. This effect was due to changes in the plasma miRNA levels either only in one of the groups or in opposite directions in both R and NR groups (Figure 3A—E, Supplementary Figure SF4). In contrast to miR-145-5p and miR-29c-3p, which did not significantly change with treatment but were predictive of treatment response at baseline, Pattern A miRNAs did not significantly differ at baseline (as evidenced by their non-significant group effects) but changed in response to short-term IIT and their changes effectively separated responders from nonresponders as assessed by PCA (Table 2, Figure 3A—F). Interestingly, the changes in let-7a-5p, miR-195-5p, miR-320b, and miR-

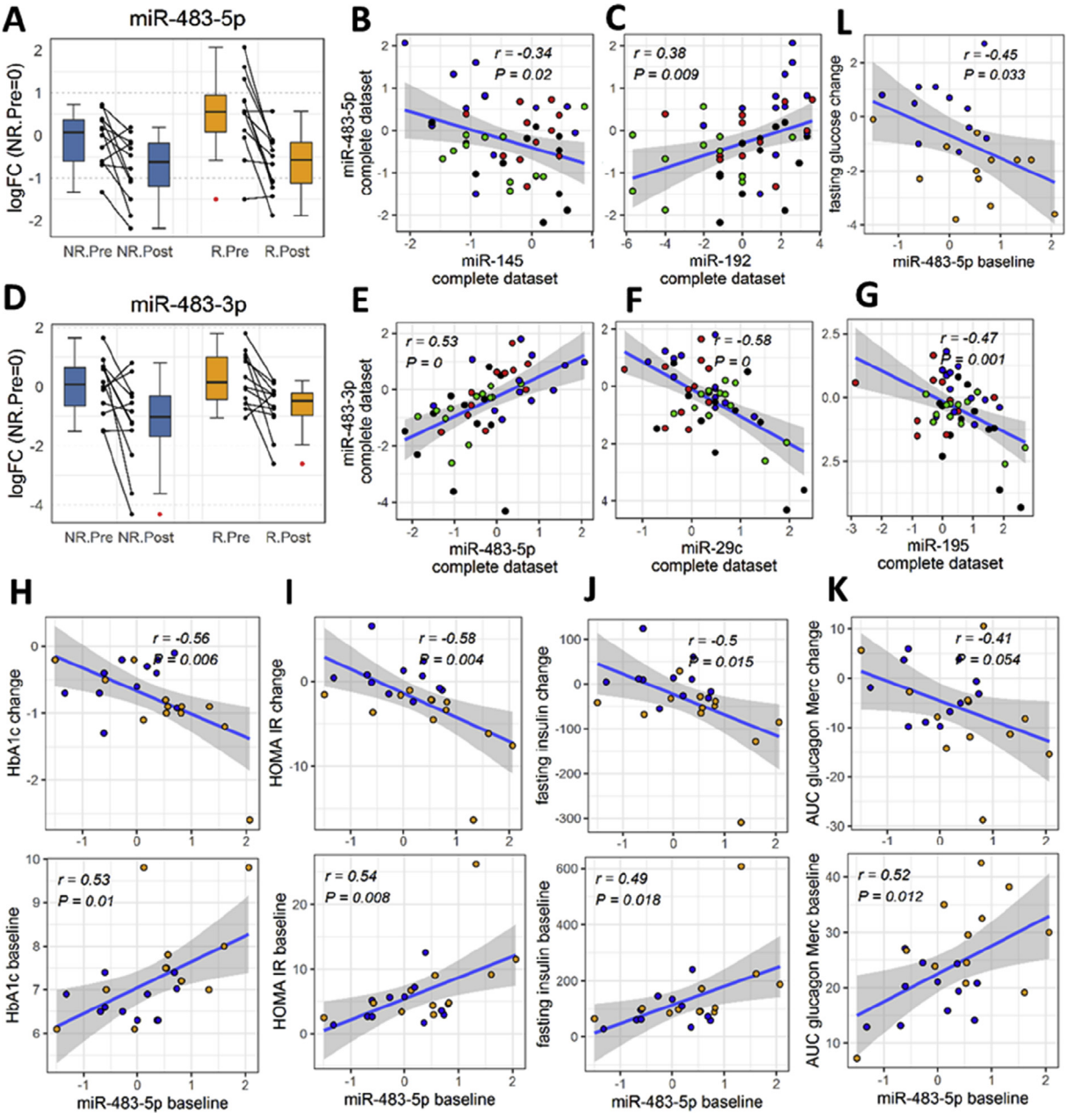

Figure 2: Expression profiling of miR-483-5p and miR-483-3p in circulation of humans with type 2 diabetes. Quantitation using real time PCR and TaqMan® assays. Measurements were normalized against the expression of the internal/endogenous control miR-191. Blue and orange circles represent nonresponder (NR) and responder (R) group data points, respectively, in panels H—L. Black, red, green, and blue represent nonresponder-post, nonresponder-pre, responder-post, and responder-pre, respectively, in panels E—G.

138-5p appear coregulated to some extent, as suggested by significant ($|r| > 0.4$, $P < 0.05$) and marginally significant ($|r| > 0.4$, $P \leq 0.062$) correlations among them (Figure 3G—I). Of note, the changes in the circulating levels of Pattern A miRNAs significantly correlated (see Figure 4) with changes in measures of β-cell function ($r_{\Delta miR.192 \sim \Delta ISSI2} = -0.51$, $P = 0.024$; $r_{\Delta miR.138 \sim \Delta(\Delta ISR0..120/\Delta gluc0..120\times} = 0.48$, $P = 0.039$; and $r_{\Delta miR.320b \sim \Delta ISSI2} = -0.48$, $P = 0.037$; all with FDR < 0.10), insulin resistance ($r_{\Delta miR.192 \sim \Delta HOMA.IR} = 0.69$, $P = 0.001$, FDR < 0.01), and fasting insulin ($r_{\Delta miR.192 \sim \Delta fasting.insulin} = 0.69$, $P = 0.001$, FDR < 0.01). The change in levels of miR-192-5p and miR-195-5p additionally tracked with the change in measures of whole body composition ($r_{\Delta miR.192 \sim \Delta Waist.circumference} = 0.56$, $P = 0.012$; $r_{\Delta miR.192 \sim \Delta BMI} = 0.46$, $P = 0.046$; and $r_{\Delta miR.195 \sim \Delta BMI} = -0.49$, $P = 0.034$, all with FDR < 0.10, Figure 4F,H). miR-195-5p displayed an additional trend with fasting glucose ($r_{\Delta miR.195 \sim \Delta fasting.glucose} = -0.44$, $P = 0.062$, FDR < 0.1). MiRNAs with a second pattern of change displaying significant Time effect but nonsignificant Group-by-Time interaction (Pattern B, Table 2, Supplementary Figures SF4 and SF5), were also identified.

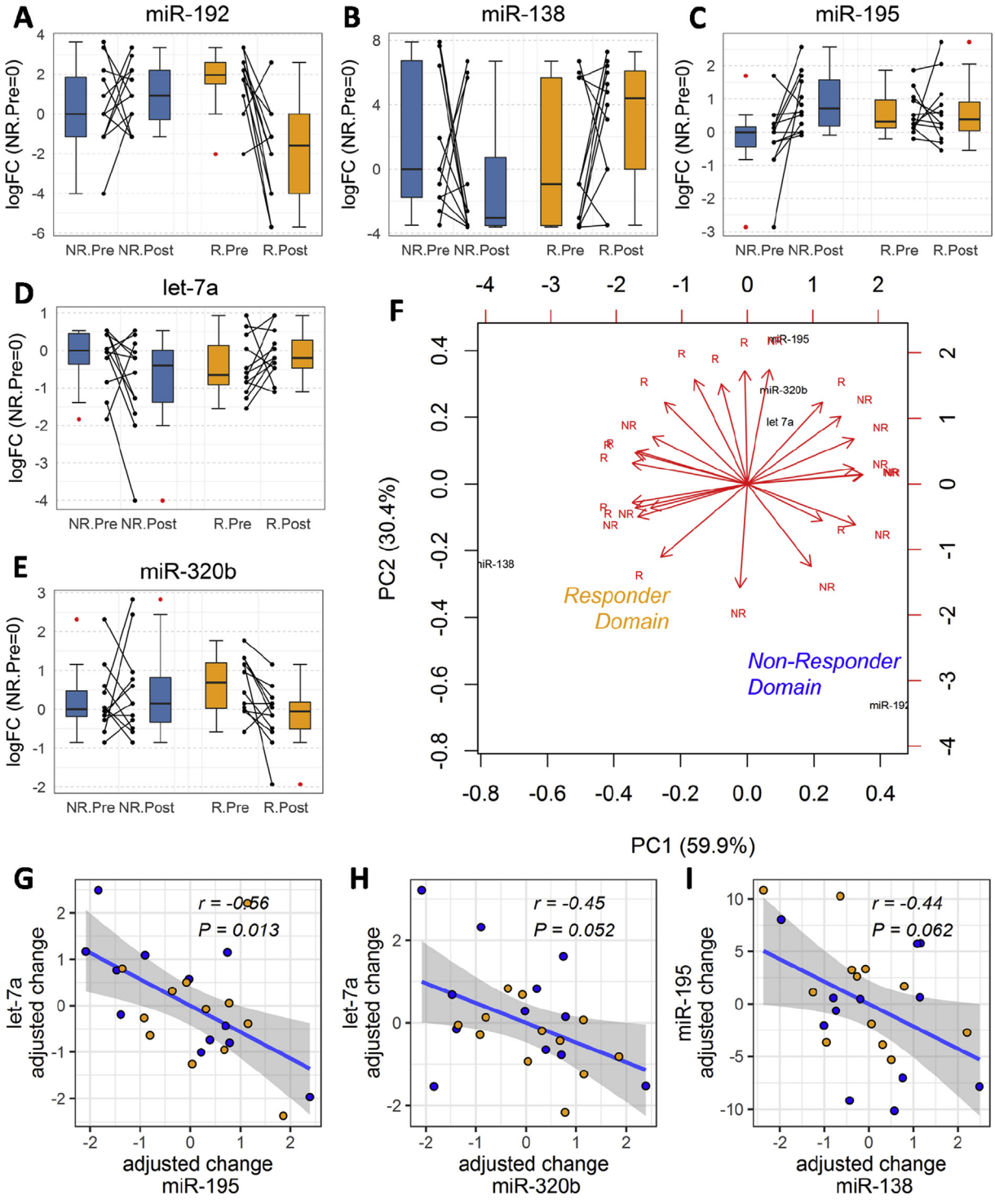

Figure 3: Longitudinal changes and correlations in microRNAs (miRNAs) that significantly change in response to short-term intensive insulin therapy (IIT). (**A**–**E**) Pattern A miRNAs with significant Group-by-Time interaction ($P < 0.05$, FDR < 0.2). Data presented as quantile-normalized log2 fold changes relative to the median of the nonresponders group at pre-IIT (NR.Pre) time point. The connected dots represent corresponding pre-therapy and post-therapy measurements for each individual participant (R: Responder group, orange filling; NR: Nonresponder group, blue filling; n = 12 per group). In the boxplots, the box delineates the first and third quartiles (the interquartile range, IQR), whereas the whiskers delineate the smallest and largest values inside a 1.5 box-length from the end of the box. The boxplot summarizes the data presented in the corresponding side-by-side dot plot, while the dot plot reveals valuable information about the longitudinal changes taking place per subject. Note that some samples have similar normalized logFC values, therefore multiple lines may converge onto a single dot. The number of lines, not the number of dots, represents the number of samples contributing data for the specific plot. Red dots represent data points located at greater than 1.5 IQR from the end of the box. Blue filling used for NR group and orange filling for R group. (**F**) Principal component analysis plot based on changes in Pattern A miRNAs effectively separate the responders from the nonresponders subjects. (**G**–**I**) Correlated changes in the circulating levels of Pattern A miRNAs in response to short-term IIT.

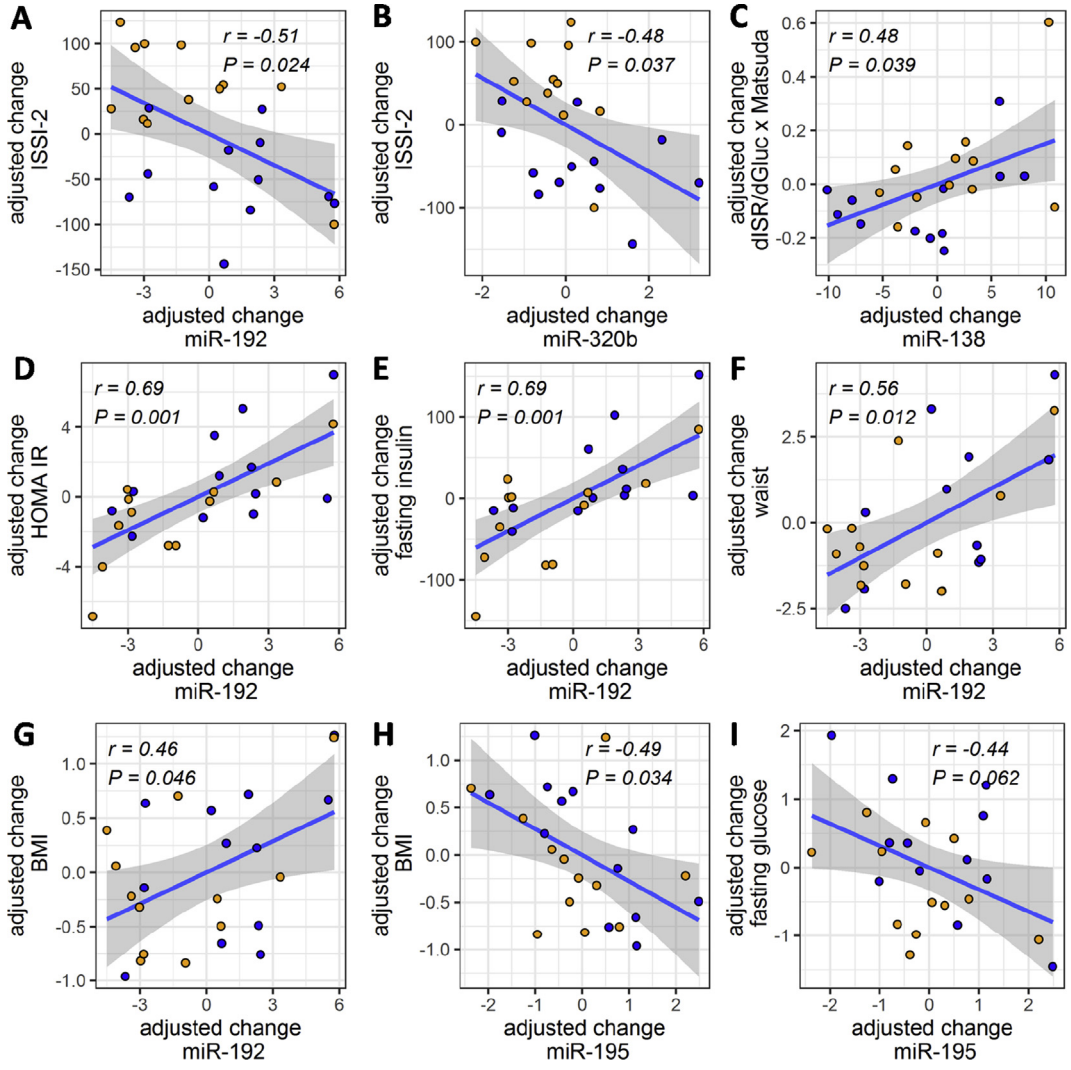

Figure 4: Correlations between changes in Pattern A circulating miRNA levels and changes in relevant clinical variables and indices of interest. Partial correlations calculated using the *ppcor* R package and adjusting for age, duration of diabetes, baseline HbA1c, and baseline AUC glucagon. Blue-filled circles represent individual values for the Nonresponder (NR) group. Orange-filled circles represent individual values for the Responder (R) group.

3.7. A network of cooperatively regulated validated miRNA targets is enriched in genes that regulate cell death and proliferation

To gain additional general mechanistic insight, we assessed the functional relevance of the putative network of genes targeted (supported by strong experimental evidence, specifically reporter assay or western blot) by both the IIT predictive and responsive miRNAs (denoted herein as IIT miRNAs). The IIT miRNA-target gene network analysis identified a total of 1672 genes that are experimentally demonstrated to physically interact with at least one of the IIT miRNAs (note that there were no targets with strong validation support in the miRTarBase database for miR-483-5p/3p —therefore, these miRNAs do not appear in our Figure 5 network). Remarkably, 109 of those (6.5%, $P = 0.0306$ as empirically determined by comparison to 10000 simulated equivalent random networks) are targeted by more than one IIT miRNAs ("cooperatively targeted") (Supplementary Table ST3). Furthermore, 91 of the cooperatively targeted genes were significantly overtargeted by the IIT miRNA set (hypergeometric $P < 0.05$ and FDR < 0.05, as compared to targeting proportions in the interaction universe/background, Supplementary Table ST3, interaction network shown in Figure 5A). Consequently, this relatively large number of overtargeted genes was also highly significant ($P = 0.0039$, as empirically determined by comparison to 10000 simulated equivalent random networks). As shown in Figures 5A and 4B, the overtargeted gene network depicted a 9-gene central cluster including BCL2, CDK6, SPTBN1, DICER1 (these four genes targeted by four IIT miRNAs each), RPS6KB1 SERPINE1, SENP1, CDC25A, and SIRT1 (these five genes targeted by three IIT miRNAs each). Gene set enrichment analysis (for GO biological processes) highlighted the enrichment in overtargeted genes that regulate cell death, cell cycle, proliferation, and cell and tissue morphogenesis, among the most relevant processes (Figure 5C,D, Supplementary Tables ST4 and ST5).

4. DISCUSSION

In this study, we provide evidence of a predictive multimodal signature in patients with early type 2 diabetes who were treated with short-term IIT. In addition, the longitudinal comparison of circulating miRNA levels between the group with considerable reversibility in beta-cell

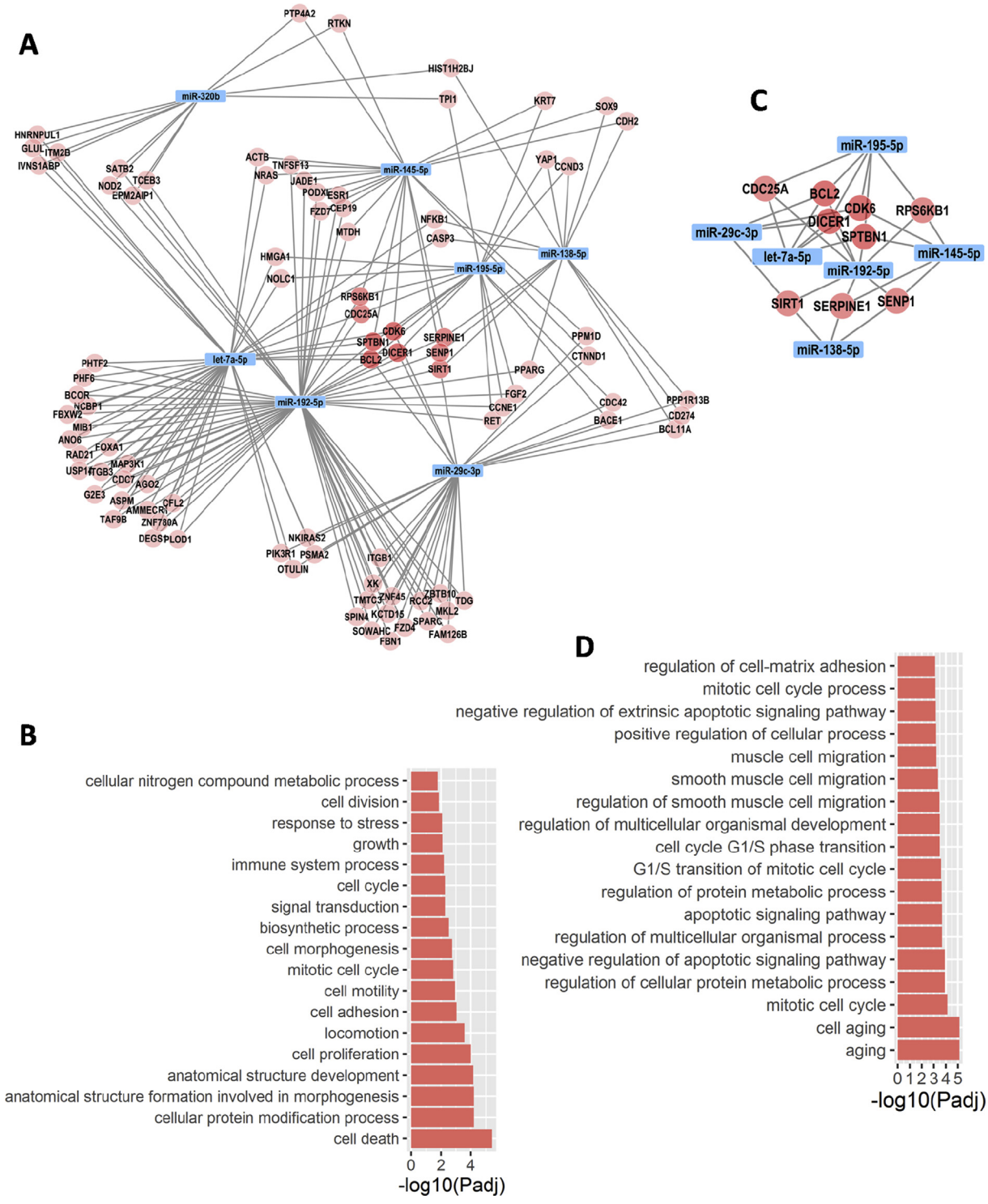

Figure 5: Functional network analysis. (**A**) Network of experimentally validated interactions between seven IIT miRNAs and corresponding 91 overtargeted genes. Overtargeted genes appear to interact with a significantly higher number of miRNAs than expected by chance (as determined by hypergeometric tests of network proportions compared to the respective proportions in the miRNA–target interaction universe/background). (**B**) Enrichment of gene ontology annotations among the complete set of 91 overtargeted genes (method set to 'slim' annotations and significance value cutoff Padj < 0.05). (**C**) Re-drawn subnetwork for the central cluster of 9 highly overtargeted genes (3 or more targeting miRNAs per gene) and interacting set of six IIT miRNAs. (**D**) Enrichment of gene ontology annotations for the central cluster of 9 overtargeted genes (method set to 'all' annotations and significance value cutoff Padj < 0.001). Categories with the lowest *P* values at the bottom of the plot. Annotation enrichment analysis was assessed using the *GOCluster_Report* function of the *systemPipeR* package in the R environment.

dysfunction in response to short-term IIT (the R group) and the group without such reversibility (the NR group), provides insights into potential underlying regulatory mechanisms determining the response to short-term IIT. A hallmark of reversibility of beta-cell dysfunction in early type 2 diabetes is the coupling of a high HbA1c with short duration of diabetes [3,5,11]. This situation arises because of the effect of glucotoxicity in amplifying the rise in glycemia that characterizes the natural history of type 2 diabetes. Specifically, early in the course of the disease, glycemia increases as beta-cell function worsens. When glucose levels reach the glucotoxic threshold at which they further compromise beta-cell function [*i.e.*, first-phase insulin secretion is abolished at blood glucose 6.4 mmol/l [54]] there will be an amplification of beta-cell dysfunction and a more rapid rise in glycemia. While the resultant effect is one of higher glycemia in early type 2 diabetes, its emergence is indicative of reversible beta-cell dysfunction (*e.g.*, due to glucotoxicity). For this reason, it was expected that, compared to nonresponders, the responders may have shorter duration of diabetes coupled with higher HbA1c.

4.1. Predictive value of baseline circulating levels of miR-145-5p, miR-29c-3p, and HbA1c

Using an implementation of the RF algorithm described by Breiman [30], which reduces bias and is protected from overfitting, we demonstrated that baseline levels of miR-145-5p, miR-29c-3p, and HbA1c could accurately and sensitively predict the response to short-term IIT. This was further evidenced by the significant correlations between miR-145-5p baseline levels and the changes in measures of beta-cell function (ISSI-2) and glycemic control (fasting glucose and HbA1c). Although these associations do not demonstrate causality, they suggest that the lower the baseline levels of miR-145-5p, the larger the increase in ISSI-2 and the larger the reduction in fasting glucose and HbA1c levels. Consistent with our findings, the parent trial found that higher baseline HbA1c levels may predict response to short-term IIT [11]. Importantly, no combination of clinical parameters demonstrated better performance than that of the multimodal RF classifier. This highlights the utility of profiling miRNA biomarkers alongside clinical parameters to predict response and aid selection of anti-diabetic therapies.

Based on validated functions of miR-145-5p (discussed below) and the correlations observed in our study, we speculate that baseline levels of this miRNA may reflect the "irreversible component" (*e.g.*, dying beta-cell mass) that affects the response to short-term IIT. Notably, expression of miR-145-5p (originally considered a cardiovascular-specific miRNA) has been found to be upregulated in the liver, muscle, and pancreas of db/db obese mice [55], to be regulated by glucose concentration and to be involved in glucose homeostasis through regulation of ABCA1 and cholesterol efflux in liver and pancreas [56], and to be upregulated by resistin (an adipocyte-derived cytokine associated with insulin resistance) both *in vivo* and *in vitro*, consequently impairing insulin signaling [57]. Other studies have found that miR-145-5p increases lipolysis in human adipocytes through increased production and processing of pro-inflammatory TNF-α [58]. Remarkably, miR-145-5p was also recently reported to induce, depending on glucose availability, either inhibitory or stimulatory effects on the apoptotic rate of hepatocellular carcinoma [52]. In that work, Lupini and colleagues demonstrated that miR-145-5p induced downregulation of [oncogenic] miR-483-3p under low-glucose and up-regulation under high-glucose conditions, which translated into induction or inhibition of miR-145-induced TP53-dependent apoptosis, respectively [52]. The authors also reported the existence of a regulatory loop between miR-145-5p and miR-483-3p in normal cells, which is lost in tumor cells. On the other hand, Mohan and colleagues reported that miR-483-5p (the mature miRNA from the forward strand) respond to elevated glucose levels and is overexpressed in pancreatic beta cells (as compared to alpha cells, both *in vitro* and *in vivo*), and that overexpression of miR-483-5p induces insulin secretion and inhibits glucagon secretion through activation of insulin signaling [53]. These authors also reported that overexpression of miR-483-5p protects against cytokine-mediated apoptosis in beta cells and is consequently elevated in prediabetic mice islets in correspondence with the increase in beta cell mass. Extrapolating to our study scenario, we hypothesize that the lower glucose levels in subjects of the nonresponder group (which are in "more advanced" stages of early type 2 diabetes, with longer duration of diabetes and with lower glycemia), together with putative higher baseline miR-145-5p tissue levels, may "reinforce" the activity of the regulatory loop by which miR-145-5p represses miR-483 (both -5p and -3p) activities, therefore augmenting the rate of miR-145-induced apoptosis and presumably the demise of beta cells in the pancreas. On the other hand, the higher levels of blood glucose in subjects in the responder group (in "earlier" stages of early type 2 diabetes, with higher glycemia due to the stronger influence of reversible glucotoxicity and lower miR-145-5p baseline levels), may induce the upregulation of miR-483 activities, which consequently counteract the pro-apoptotic functions of miR-145 and presumably stimulates proliferation of beta cells in the pancreas. The consequent improvement in beta cell function in the responder group would then contribute to reversing glucotoxicity and lowering glycemic levels, consequently inducing the observed rising trend in miR-145-5p and correspondingly decreasing trend in miR-483-5p after short-term IIT. We hypothesize that the balanced interplay among these miRNAs and respective regulated genes, in a tissue-specific physiological/pathophysiological context are important determinants of disease progression and response to therapy in subjects with type 2 diabetes. These results represent an indirect validation of the occurrence of the regulatory loop between miR-145-5p and miR-483-3p/5p in tissues (likely the pancreas and/or liver) from humans with type 2 diabetes and indicate that baseline levels of miR-483-5p in circulation can also be predictive of the response to short-term IIT. Furthermore, Cui and colleagues recently demonstrated that downregulation of miR-145-5p in diabetes-bone marrow stromal-cells (diabetes-BMSCs) increased cell proliferation and decreased cell death in addition to improving vascular remodeling in the ischemic rat brain [59]. We speculate that, in a somewhat similar fashion, people with type 2 diabetes that have lower levels of miR-145-5p (as in our R group) may experience reduced beta-cell death, improved proliferation, and an improved vasculogenic microenvironment in the pancreas that, therefore, may elicit a positive response to short-term IIT. On the other hand, miR-29, one of the most abundant miRNA family in human pancreatic β-cells and in the liver [60], has been reported to be downregulated under hyperinsulinemic conditions (*e.g.*, in the heart, possibly as an adaptive mechanism to protect the organ in the prediabetic stage [61]), but increased in response to loss of hyperinsulinemia and elevated plasma glucose levels [62]. However, an apparent inverse correlation between liver and circulating plasma miR-29 levels in type 2 diabetes has also been suggested and deemed intriguing [63]. Although miR-29 did not show significant correlations with relevant clinical measurements in our subjects, we note that responders tend to have higher baseline levels of circulating miR-29. Therefore, considering the reported inverse correlation between circulating and tissue levels for miR-29 in type 2 diabetes, we speculate that responders may have lower levels of miR-29 in some insulin-sensitive tissues, which may provide for additional protection in these subjects and a positive response to the treatment.

4.2. Differential miRNA signature responsive to short-term IIT

Five circulating miRNAs, miR-138-5p, miR-192-5p, miR-195-5p, miR-320b, and let-7a-5p, showed significant differential expression changes in response to four-week short-term IIT. Their changes in the subjects' circulation effectively separated the subjects that responded to the therapy from those that did not, as assessed by PCA. This suggests that short-term IIT induced major changes in the circulating levels of pattern A miRNAs that are defined by the subjects' capacity to respond to the therapy. Those changes also associated with concomitant changes in beta-cell function (as evidenced by significant correlation with the change in ISSI-2), insulin resistance (as evidenced by significant correlation with the change in HOMA IR), and fasting insulin concentrations. This suggests that Pattern A miRNAs may regulate a reversible state, potentially due to glucotoxicity, that is responsive to short-term IIT in people with early type 2 diabetes.

Notably, binding of miR-138-5p to the TATA-box region in the promoter of the insulin gene enhances the promoter activity and consequently the expression of the insulin gene [64]. Therefore, the elevated plasma abundance detected for miR-138-5p in our R group suggests that short-term IIT may increase the expression of the insulin gene in pancreatic beta-cells. On the other hand, miR-192-5p is one of the most abundant miRNAs in pancreatic beta-cells, liver, and kidney [65,66], and is significantly increased in the circulation in early disease stages, as in people with prediabetes [67]. In addition, roles in insulin resistance, cardiometabolic phenotypes, diabetic nephropathy, and non-alcoholic fatty liver disease (NAFLD) have recently been suggested [68–70]. Notably, we recently identified miR-192-5p as a key vitamin D-responsive miRNA in subjects with prediabetes [50]. Supporting our findings in this study, miR-192-5p was also reduced by the vitamin D treatment and correlated with the change in fasting plasma glucose [50]. Another subset of Pattern A miRNAs, namely let-7a-5p, miR-195-5p, and miR-320b appeared to be coregulated, as suggested by the significant correlations among them. Consistent with this notion, these three miRNAs have been similarly implicated in diabetes [23,71–77], cardiovascular disease [74,77–79], and cancer [80–83], and their effects appear to be associated with the miRNA presence in exosomes [73–76,80]. Consistent with our findings, let-7a-5p (a highly abundant miRNA in human β-cells [84]) was found to be significantly downregulated in plasma exosomes from people with type 2 diabetes, significantly correlated with plasma glucose and HbA1c levels, and responsive to antidiabetic treatment [75]. On the other hand, miR-195-5p was found upregulated in the liver of diabetic rats and its expression showed a linear relationship with the glycemic phenotype of three distinct strains, which suggested a role in the pathophysiology of type 2 diabetes [72]. Remarkably, we have recently detected circulating exosomal miR-195-5p changing in diabetic people in response to treatment with pioglitazone [85]. Regarding miR-320b, its upregulation in cultured adipocytes contributed to the development of insulin resistance [71] while in diabetic mice contributed to the development of hyperglycemic/metabolic memory in the heart despite normoglycemia restoration [77]. In addition, family member miR-320a was found to regulate skeletal muscle mitochondrial metabolism [86]. These findings suggest potential clinical utility for the design of new strategies to interfere with the development of hyperglycemic memory in specific tissues. We hypothesize that the implementation of short-term IIT early in the development of type 2 diabetes could contribute to reducing the levels of miR-320b and consequently, interfere with the development of hyperglycemic memory later in the course of the disease, potentially contributing to reduced risk of disease progression and reduced risk of cardiovascular complications, as evidenced in the United Kingdom Prospective Diabetes Study [87].

Collectively, the predictive and responsive miRNAs (IIT miRNAs) define a network of validated miRNA–mRNA interactions that additionally suggests the coordinated regulation of genes that regulate cell proliferation, apoptosis, and cell/tissue morphogenesis. A central cluster of nine overtargeted genes including BCL2, CDK6, SPTBN1, DICER1, RPS6KB1 SERPINE1, SENP1, CDC25A, and SIRT1 (identified from among 91 genes targeted by more than one of the select IIT miRNAs) emerge as potentially key players driving a positive response to the insulin therapy in early diabetic patients. Reduced demise of challenged/dying beta-cells and concomitant enhanced beta-cell proliferation and pancreatic tissue remodeling (morphogenesis) in the diabetic pancreas is a plausible mechanism that could explain, at least in part, the beneficial and long-term effects of short-term IIT in humans with early type 2 diabetes. Interestingly, a recent trans-omic network analysis of selective responses to low (basal) and high (induced) insulin administration (*in vitro* using rat hepatoma cells and *in vivo* using insulin-clamped rat livers) found that basal and induced insulin effects are decoded by the cells via mostly mutually exclusive pathways [88]. However, FoxO1, a key transcription factor inhibited by Akt phosphorylation and activated by Sirt1 deacetylation among other stimuli [89], was able to regulate both basal and induced insulin-responsive transcripts [88]. As SIRT1, which has also been found to be a critical factor for Pdx1 transcription and β cell formation [90], is one of the most significantly overtargeted genes in our analysis and FOXA1 (also activated by Sirt1 and an interdependent binding partner and enhancer of FoxO1 binding to the promoter of insulin-sensitive genes [91]) is also significantly overtargeted by IIT miRNAs (refer to Figure 5 networks and Supplementary Table ST3), these results suggest that IIT miRNAs may be functionally involved in the regulation of both the basal and induced cellular responses to insulin. Consequently, deregulation and/or individual variation in IIT miRNA levels may impact the natural history of type 2 diabetes and/or the heterogeneity in response to treatment.

Also notably, DICER1, one of the top overtargeted genes in our network analysis (targeted by 4 of the 7 IIT miRNAs), was recently shown by the Kahn group to play a fundamental role in adipose tissue, which contributes a majority of exosomal miRNAs into the circulation [92]. Additionally, DICER-dependent miRNA biogenesis was shown to be critical to sustain survival and activity of POMC neurons and to mediate hypothalamic regulation of energy balance by relaying peripheral nutrient excess and/or obesity [93,94]. Of note, the IIT miRNAs also significantly overtarget the PPARG transcript (Figure 5A), which is a master transcriptional regulator of metabolism and, in particular, critical for fat-cell formation/differentiation of adipose tissue [95–97]. Importantly, a recent work by Taylor and collaborators demonstrated that substantial (15%) weight loss through a low-calorie diet in subjects with type 2 diabetes can lead to restoration of β cell function in about 2/3 of the intervened population [98]. These authors found that the major difference between their responder and nonresponder groups was the respective ability to recover first-phase insulin response (response to the intervention was then dependent upon the capacity of β cell recovery) and, as in our cohort, that response was predicted by shorter duration of diabetes. Those results, in the context of our work and the work of others discussed here, support the hypothesis that short-term IIT and significant weight loss interventions may similarly improve β cell function, possibly via alterations in adipocyte miRNA release, and contribute to remission of type 2 diabetes.

Pattern B miRNAs, which show a significant Time effect generally due to similar directional changes in both R and NR groups, appear to represent miRNAs modulated by the insulin therapy or glycemia but not causally related to the improvements in insulin secretion and sensitivity evidenced by the change in the ISSI-2 index. These miRNAs may be responsible, at least in part, for the significant reduction of HbA1c

levels in both groups. Supporting this reasoning, we and others have previously found several of the Pattern B miRNAs changing in the circulation of people with obesity and/or diabetes (*e.g.*, miR-34a, miR-144, let-7b [18,19,22,24,51,99]), and playing mechanistic roles in obesity and glucose metabolism (*e.g.*, miR-15b, miR-802 [100,101]). Although we consider these results exciting and promising, there are several limitations in our study. First, the limited cohort size makes validation in independent cohorts important. Second, our study involved people with type 2 diabetes in an early stage in the natural history of the disease, therefore limiting the generalizability to other disease stages. In addition, direct experimental validation of target gene changes and mRNA knockdown/overexpression in human diabetic tissue samples is lacking, which could strengthen our findings by clarifying potential mechanisms. It is not clear, for example, whether the between group differences in the change in miRNA abundance are causally related to changes in blood glucose, insulin secretion, insulin resistance, or changes in some other unmeasured factors. Lastly, beta-cell function and insulin resistance were assessed with OGTT-based surrogate indices instead of with "gold standard" clamp measurements. However, ISSI-2 and HOMA-IR indexes are well-validated measurements used in previous studies [11].

5. CONCLUSIONS

In this study, we have generated an accurate multimodal RF classifier with potential clinical utility for predicting responses to short-term IIT among patients with recently diagnosed type 2 diabetes. An important current limitation of short-term IIT is the inability to identify potential responders at baseline. Therefore, we emphasize the potential clinical relevance of our study, as it represents a first step in that context and provides key insight into the pathophysiologic determinants of reversibility of beta-cell dysfunction. Such reversibility cannot be identified by any other conventional measure in use today. This insight may inform targeted therapeutic interventions aimed at ameliorating reversible beta-cell dysfunction and thereby changing the natural history of type 2 diabetes. Whether the specific miRNAs and RF classifier will also be useful to predict responses to antidiabetic therapies is an intriguing question warranting further study.

ACKNOWLEDGMENTS

We would like to thank Florida Hospital for granting funds to A.S. and R.E.P. to conduct this study. The LIBRA trial (parent study) was funded by Novo Nordisk as an investigator-initiated trial to R.R. and B.Z. R.R holds the Boehringer Ingelheim Chair in Beta-cell Preservation, Function and Regeneration at Mount Sinai Hospital.

AUTHOR CONTRIBUTIONS

A.A.S, R.R., and REP contributed to the conception and design of the research design, analysis plan, supervision of the analysis, study implementation, data acquisition, and interpretation, writing of the manuscript, and critical revision and final approval of the manuscript. Y.O.N.L performed experiments, conducted data analysis, and contributed to data interpretation and writing of the manuscript. R.E.P and B.Z. contributed to the study design, study implementation, data interpretation, and critical revision and final approval of the manuscript. A.A.S is the guarantor of this work and, as such, had full access to all the data in the study and takes responsibility for the integrity of the data and the accuracy of the data analysis.

PRIOR PRESENTATION

None.

CONFLICT OF INTERESTS/DISCLOSURE SUMMARY

This study was funded by startup funds granted to A.S. and R.E.P by Florida Hospital. The LIBRA trial was funded by Novo Nordisk as an investigator-initiated trial to R.R. and B.Z.. R.R. and B.Z. have received consulting honoraria and research support from Novo Nordisk. REP has received research grants (to his institution) from Lexicon Pharmaceuticals, Ligand Pharmaceuticals, Inc., Lilly, Merck, Novo Nordisk, Sanofi-Aventis US, LLC, and Takeda and has previously received speaker and/or consultancy fees (to his institution) from AstraZeneca, Boehringer Ingelheim, Eisai, Inc., GlaxoSmithKline, Hanmi Pharmaceutical Co., Ltd., Janssen Scientific Affairs, LLC, Ligand Pharmaceuticals, Inc., Lilly, Merck, Novo Nordisk, Pfizer, Sanofi and Takeda. No other potential conflicts of interest relevant to this article were reported.

APPENDIX A. SUPPLEMENTARY DATA

Supplementary data to this article can be found online at https://doi.org/10.1016/j.molmet.2018.11.003.

REFERENCES

[1] Kahn, S.E., Zraika, S., Utzschneider, K.M., Hull, R.L., 2009. The beta cell lesion in type 2 diabetes: there has to be a primary functional abnormality. Diabetologia 52:1003–1012.
[2] Wajchenberg, B.L., 2007. beta-cell failure in diabetes and preservation by clinical treatment. Endocrine Reviews 28:187–218.
[3] Retnakaran, R., Zinman, B., 2012. Short-term intensified insulin treatment in type 2 diabetes: long-term effects on beta-cell function. Diabetes, Obesity & Metabolism 14(Suppl 3):161–166.
[4] Kramer, C.K., Choi, H., Zinman, B., Retnakaran, R., 2014. Glycemic variability in patients with early type 2 diabetes: the impact of improvement in beta-cell function. Diabetes Care 37:1116–1123.
[5] Weng, J., Retnakaran, R., Ariachery, C.A., Ji, L., Meneghini, L., Yang, W., et al., 2015. Short-term intensive insulin therapy at diagnosis in type 2 diabetes: plan for filling the gaps. Diabetes/Metabolism Research and Reviews 31:537–544.
[6] Ryan, E.A., Imes, S., Wallace, C., 2004. Short-term intensive insulin therapy in newly diagnosed type 2 diabetes. Diabetes Care 27:1028–1032.
[7] Li, Y., Xu, W., Liao, Z., Yao, B., Chen, X., Huang, Z., et al., 2004. Induction of long-term glycemic control in newly diagnosed type 2 diabetic patients is associated with improvement of beta-cell function. Diabetes Care 27:2597–2602.
[8] Weng, J., Li, Y., Xu, W., Shi, L., Zhang, Q., Zhu, D., et al., 2008. Effect of intensive insulin therapy on beta-cell function and glycaemic control in patients with newly diagnosed type 2 diabetes: a multicentre randomised parallel-group trial. Lancet (London, England) 371:1753–1760.
[9] Wallia, A., Molitch, M.E., 2014. Insulin therapy for type 2 diabetes mellitus. Journal of the American Medical Association 311:2315–2325.
[10] Kramer, C.K., Zinman, B., Retnakaran, R., 2013. Short-term intensive insulin therapy in type 2 diabetes mellitus: a systematic review and meta-analysis. The Lancet Diabetes & Endocrinology 1:28–34.
[11] Kramer, C.K., Choi, H., Zinman, B., Retnakaran, R., 2013. Determinants of reversibility of beta-cell dysfunction in response to short-term intensive insulin therapy in patients with early type 2 diabetes. American Journal of Physiology Endocrinology and Metabolism 305:E1398–E1407.
[12] Retnakaran, R., Yakubovich, N., Qi, Y., Opsteen, C., Zinman, B., 2010. The response to short-term intensive insulin therapy in type 2 diabetes. Diabetes, Obesity & Metabolism 12:65–71.
[13] Sayed, D., Abdellatif, M., 2011. MicroRNAs in development and disease. Physiological Reviews 91:827–887.
[14] Victoria, B., Nunez Lopez, Y.O., Masternak, M.M., 2017. MicroRNAs and the metabolic hallmarks of aging. Molecular and Cellular Endocrinology 455:131–147.

[15] Shantikumar, S., Caporali, A., Emanueli, C., 2012. Role of microRNAs in diabetes and its cardiovascular complications. Cardiovascular Research 93: 583–593.

[16] Guay, C., Regazzi, R., 2015. Role of islet microRNAs in diabetes: which model for which question? Diabetologia 58:456–463.

[17] Prats-Puig, A., Ortega, F.J., Mercader, J.M., Moreno-Navarrete, J.M., Moreno, M., Bonet, N., et al., 2013. Changes in circulating microRNAs are associated with childhood obesity. The Journal of Clinical Endocrinology and Metabolism 98:E1655–E1660.

[18] Nunez Lopez, Y.O., Garufi, G., Seyhan, A.A., 2016. Altered levels of circulating cytokines and microRNAs in lean and obese individuals with prediabetes and type 2 diabetes. Molecular BioSystems 13:106–121.

[19] Jones, A., Danielson, K.M., Benton, M.C., Ziegler, O., Shah, R., Stubbs, R.S., et al., 2017. miRNA signatures of insulin resistance in obesity. Obesity (Silver Spring, Md) 25:1734–1744.

[20] Nunez Lopez, Y.O., Garufi, G., Pasarica, M., Seyhan, A.A., 2018. Elevated and correlated expressions of miR-24, miR-30d, miR-146a, and SFRP-4 in human abdominal adipose tissue play a role in adiposity and insulin resistance. International Journal of Endocrinology 2018:7.

[21] Ortega, F.J., Mercader, J.M., Catalan, V., Moreno-Navarrete, J.M., Pueyo, N., Sabater, M., et al., 2013. Targeting the circulating microRNA signature of obesity. Clinical Chemistry 59:781–792.

[22] Zampetaki, A., Kiechl, S., Drozdov, I., Willeit, P., Mayr, U., Prokopi, M., et al., 2010. Plasma microRNA profiling reveals loss of endothelial miR-126 and other microRNAs in type 2 diabetes. Circulation Research 107:810–817.

[23] Ortega, F.J., Mercader, J.M., Moreno-Navarrete, J.M., Rovira, O., Guerra, E., Esteve, E., et al., 2014. Profiling of circulating microRNAs reveals common microRNAs linked to type 2 diabetes that change with insulin sensitization. Diabetes Care 37:1375–1383.

[24] Seyhan, A.A., Nunez Lopez, Y.O., Xie, H., Yi, F., Mathews, C., Pasarica, M., et al., 2016. Pancreas-enriched miRNAs are altered in the circulation of subjects with diabetes: a pilot cross-sectional study. Scientific Reports 6: 31479.

[25] He, Y., Ding, Y., Liang, B., Lin, J., Kim, T.K., Yu, H., et al., 2017. A systematic study of dysregulated microRNA in type 2 diabetes mellitus. International Journal of Molecular Sciences 18.

[26] Copier, C.U., León, L., Fernández, M., Contador, D., Calligaris, S.D., 2017. Circulating miR-19b and miR-181b are potential biomarkers for diabetic cardiomyopathy. Scientific Reports 7.

[27] Catanzaro, G., Besharat, Z.M., Chiacchiarini, M., Abballe, L., Sabato, C., Vacca, A., et al., 2018. Circulating microRNAs in elderly type 2 diabetic patients. International Journal of Endocrinology 2018:11.

[28] Retnakaran, R., Kramer, C.K., Choi, H., Swaminathan, B., Zinman, B., 2014. Liraglutide and the preservation of pancreatic beta-cell function in early type 2 diabetes: the LIBRA trial. Diabetes Care 37:3270–3278.

[29] Kramer, C.K., Zinman, B., Choi, H., Connelly, P.W., Retnakaran, R., 2017. Impact of the glucagon assay when assessing the effect of chronic liraglutide therapy on glucagon secretion. The Journal of Clinical Endocrinology and Metabolism.

[30] Breiman, L., 2001. Random forests. Machine Learning 45:5–32.

[31] R Core Team, 2018. R: a language and environment for statistical computing. Vienna, Austria: R Foundation for Statistical Computing.

[32] Kirschner, M.B., Edelman, J.B., Kao, S.C.H., Vallely, M.P., van Zandwijk, N., Reid, G., 2013. The impact of hemolysis on cell-free microRNA biomarkers. Frontiers in Genetics 4:94.

[33] Shah, J.S., Soon, P.S., Marsh, D.J., 2016. Comparison of methodologies to detect low levels of hemolysis in serum for accurate assessment of serum microRNAs. PLoS One 11:e0153200.

[34] Blondal, T., Jensby Nielsen, S., Baker, A., Andreasen, D., Mouritzen, P., Wrang Teilum, M., et al., 2013. Assessing sample and miRNA profile quality in serum and plasma or other biofluids. Methods (San Diego, Calif) 59:S1–S6.

[35] Strobl, C., Malley, J., Tutz, G., 2009. An introduction to recursive partitioning: rationale, application and characteristics of classification and regression trees, bagging and random forests. Psychological Methods 14:323–348.

[36] Marinic, I., Supek, F., Kovacic, Z., Rukavina, L., Jendricko, T., Kozaric-Kovacic, D., 2007. Posttraumatic stress disorder: diagnostic data analysis by data mining methodology. Croatian Medical Journal 48:185–197.

[37] Liaw, A., Wiener, M., 2002. Classification and regression by randomForest. R News 2.

[38] Díaz-Uriarte, R., Alvarez de Andrés, S., 2006. Gene selection and classification of microarray data using random forest. BMC Bioinformatics 7:3.

[39] Laurent, L.C., Chen, J., Ulitsky, I., Mueller, F.J., Lu, C., Shamir, R., et al., 2008. Comprehensive microRNA profiling reveals a unique human embryonic stem cell signature dominated by a single seed sequence. Stem cells (Dayton, Ohio) 26:1506–1516.

[40] Lewohl, J.M., Nunez, Y.O., Dodd, P.R., Tiwari, G.R., Harris, R.A., Mayfield, R.D., 2011. Up-regulation of microRNAs in brain of human alcoholics. Alcoholism: Clinical and Experimental Research 35:1928–1937.

[41] Xiao, Y., Xu, C., Guan, J., Ping, Y., Fan, H., Li, Y., et al., 2012. Discovering dysfunction of multiple microRNAs cooperation in disease by a conserved microRNA co-expression network. PLoS One 7:e32201.

[42] Nunez, Y.O., Truitt, J.M., Gorini, G., Ponomareva, O.N., Blednov, Y.A., Harris, R.A., et al., 2013. Positively correlated miRNA-mRNA regulatory networks in mouse frontal cortex during early stages of alcohol dependence. BMC Genomics 14:725.

[43] Gorini, G., Nunez, Y.O., Mayfield, R.D., 2013. Integration of miRNA and protein profiling reveals coordinated neuroadaptations in the alcohol-dependent mouse brain. PLoS One 8:e82565.

[44] Victoria Martinez, B., Dhahbi, J.M., Nunez Lopez, Y.O., Lamperska, K., Golusinski, P., Luczewski, L., et al., 2015. Circulating small non-coding RNA signature in head and neck squamous cell carcinoma. Oncotarget 6:19246–19263.

[45] Victoria, B., Dhahbi, J.M., Nunez Lopez, Y.O., Spinel, L., Atamna, H., Spindler, S.R., et al., 2015. Circulating microRNA signature of genotype-by-age interactions in the long-lived Ames dwarf mouse. Aging Cell 14:1055–1066.

[46] Shao, T., Wang, G., Chen, H., Xie, Y., Jin, X., Bai, J., et al., 2018. Survey of miRNA-miRNA cooperative regulation principles across cancer types. Briefings in Bioinformatics.

[47] Cava, C., Colaprico, A., Bertoli, G., Graudenzi, A., Silva, T.C., Olsen, C., et al., 2017. SpidermiR: an R/bioconductor package for integrative analysis with miRNA data. International Journal of Molecular Sciences 18:274.

[48] Demchak, B., Hull, T., Reich, M., Liefeld, T., Smoot, M., Ideker, T., et al., 2014. Cytoscape: the network visualization tool for GenomeSpace workflows. F1000Research 3:151.

[49] Backman, T.W.H., Girke, T., 2016. systemPipeR: NGS workflow and report generation environment. BMC Bioinformatics 17:388.

[50] Nunez Lopez, Y.O., Pittas, A.G., Pratley, R.E., Seyhan, A.A., 2017. Circulating levels of miR-7, miR-152 and miR-192 respond to vitamin D supplementation in adults with prediabetes and correlate with improvements in glycemic control. The Journal of Nutritional Biochemistry 49:117–122.

[51] Nunez Lopez, Y.O., Coen, P.M., Goodpaster, B.H., Seyhan, A.A., 2017. Gastric bypass surgery with exercise alters plasma microRNAs that predict improvements in cardiometabolic risk. International Journal of Obesity 41: 1121–1130.

[52] Lupini, L., Pepe, F., Ferracin, M., Braconi, C., Callegari, E., Pagotto, S., et al., 2016. Over-expression of the miR-483-3p overcomes the miR-145/TP53 pro-apoptotic loop in hepatocellular carcinoma. Oncotarget 7:31361–31371.

[53] Mohan, R., Mao, Y., Zhang, S., Zhang, Y.W., Xu, C.R., Gradwohl, G., et al., 2015. Differentially expressed microRNA-483 confers distinct functions in pancreatic beta- and alpha-cells. Journal of Biological Chemistry 290: 19955–19966.

[54] Brunzell, J.D., Robertson, R.P., Lerner, R.L., Hazzard, W.R., Ensinck, J.W., Bierman, E.L., et al., 1976. Relationships between fasting plasma glucose levels and insulin secretion during intravenous glucose tolerance tests. The Journal of Clinical Endocrinology and Metabolism 42:222–229.

[55] Jordan, S.D., Kruger, M., Willmes, D.M., Redemann, N., Wunderlich, F.T., Bronneke, H.S., et al., 2011. Obesity-induced overexpression of miRNA-143 inhibits insulin-stimulated AKT activation and impairs glucose metabolism. Nature Cell Biology 13:434–446.

[56] Kang, M.H., Zhang, L.H., Wijesekara, N., de Haan, W., Butland, S., Bhattacharjee, A., et al., 2013. Regulation of ABCA1 protein expression and function in hepatic and pancreatic islet cells by miR-145. Arteriosclerosis, Thrombosis, and Vascular Biology 33:2724–2732.

[57] Wen, F., Yang, Y., Jin, D., Sun, J., Yu, X., Yang, Z., 2014. MiRNA-145 is involved in the development of resistin-induced insulin resistance in HepG2 cells. Biochemical and Biophysical Research Communications 445:517–523.

[58] Lorente-Cebrian, S., Mejhert, N., Kulyte, A., Laurencikiene, J., Astrom, G., Heden, P., et al., 2014. MicroRNAs regulate human adipocyte lipolysis: effects of miR-145 are linked to TNF-alpha. PLoS One 9:e86800.

[59] Cui, C., Ye, X., Chopp, M., Venkat, P., Zacharek, A., Yan, T., et al., 2016. miR-145 regulates diabetes-bone marrow stromal cell-induced neurorestorative effects in diabetes stroke rats. Stem Cells Translational Medicine 5:1656–1667.

[60] Dooley, J., Garcia-Perez, J.E., Sreenivasan, J., Schlenner, S.M., Vangoitsenhoven, R., Papadopoulou, A.S., et al., 2016. The microRNA-29 family dictates the balance between homeostatic and pathological glucose handling in diabetes and obesity. Diabetes 65:53–61.

[61] Arnold, N., Koppula, P.R., Gul, R., Luck, C., Pulakat, L., 2014. Regulation of cardiac expression of the diabetic marker microRNA miR-29. PLoS One 9: e103284.

[62] Slusarz, A., Pulakat, L., 2015. The two faces of miR-29. Journal of Cardiovascular Medicine (Hagerstown, Md) 16:480–490.

[63] Kurtz, C.L., Peck, B.C., Fannin, E.E., Beysen, C., Miao, J., Landstreet, S.R., et al., 2014. MicroRNA-29 fine-tunes the expression of key FOXA2-activated lipid metabolism genes and is dysregulated in animal models of insulin resistance and diabetes. Diabetes 63:3141–3148.

[64] Zhang, Y., Fan, M., Zhang, X., Huang, F., Wu, K., Zhang, J., et al., 2014. Cellular microRNAs up-regulate transcription via interaction with promoter TATA-box motifs. RNA (New York, NY) 20:1878–1889.

[65] van de Bunt, M., Gaulton, K.J., Parts, L., Moran, I., Johnson, P.R., Lindgren, C.M., et al., 2013. The miRNA profile of human pancreatic islets and beta-cells and relationship to type 2 diabetes pathogenesis. PLoS One 8: e55272.

[66] Sun, Y., Koo, S., White, N., Peralta, E., Esau, C., Dean, N.M., et al., 2004. Development of a micro-array to detect human and mouse microRNAs and characterization of expression in human organs. Nucleic Acids Research 32: e188.

[67] Parrizas, M., Brugnara, L., Esteban, Y., Gonzalez-Franquesa, A., Canivell, S., Murillo, S., et al., 2014. Circulating miR-192 and miR-193b are markers of prediabetes and are modulated by an exercise intervention. The Journal of Clinical Endocrinology and Metabolism jc20142574.

[68] Shah, R., Murthy, V., Pacold, M., Danielson, K., Tanriverdi, K., Larson, M.G., et al., 2017. Extracellular RNAs are associated with insulin resistance and metabolic phenotypes. Diabetes Care 40:546–553.

[69] Kato, M., Zhang, J., Wang, M., Lanting, L., Yuan, H., Rossi, J.J., et al., 2007. MicroRNA-192 in diabetic kidney glomeruli and its function in TGF-beta-induced collagen expression via inhibition of E-box repressors. Proceedings of the National Academy of Sciences of the United States of America 104: 3432–3437.

[70] Pirola, C.J., Fernandez Gianotti, T., Castano, G.O., Mallardi, P., San Martino, J., Mora Gonzalez Lopez Ledesma, M., et al., 2015. Circulating microRNA signature in non-alcoholic fatty liver disease: from serum non-coding RNAs to liver histology and disease pathogenesis. Gut 64:800–812.

[71] Ling, H.Y., Ou, H.S., Feng, S.D., Zhang, X.Y., Tuo, Q.H., Chen, L.X., et al., 2009. Changes in microRNA (miR) profile and effects of miR-320 in insulin-resistant 3T3-L1 adipocytes. Clinical and Experimental Pharmacology & Physiology 36:e32–e39.

[72] Herrera, B.M., Lockstone, H.E., Taylor, J.M., Ria, M., Barrett, A., Collins, S., et al., 2010. Global microRNA expression profiles in insulin target tissues in a spontaneous rat model of type 2 diabetes. Diabetologia 53:1099–1109.

[73] Karolina, D.S., Tavintharan, S., Armugam, A., Sepramaniam, S., Pek, S.L., Wong, M.T., et al., 2012. Circulating miRNA profiles in patients with metabolic syndrome. The Journal of Clinical Endocrinology and Metabolism 97: E2271–E2276.

[74] Wang, X., Huang, W., Liu, G., Cai, W., Millard, R.W., Wang, Y., et al., 2014. Cardiomyocytes mediate anti-angiogenesis in type 2 diabetic rats through the exosomal transfer of miR-320 into endothelial cells. Journal of Molecular and Cellular Cardiology 74:139–150.

[75] Santovito, D., De Nardis, V., Marcantonio, P., Mandolini, C., Paganelli, C., Vitale, E., et al., 2014. Plasma exosome microRNA profiling unravels a new potential modulator of adiponectin pathway in diabetes: effect of glycemic control. The Journal of Clinical Endocrinology and Metabolism 99:E1681–E1685.

[76] Guay, C., Menoud, V., Rome, S., Regazzi, R., 2015. Horizontal transfer of exosomal microRNAs transduce apoptotic signals between pancreatic beta-cells. Cell Communication and Signaling 13:17.

[77] Costantino, S., Paneni, F., Luscher, T.F., Cosentino, F., 2016. MicroRNA profiling unveils hyperglycaemic memory in the diabetic heart. European Heart Journal 37:572–576.

[78] Marques, F.Z., Vizi, D., Khammy, O., Mariani, J.A., Kaye, D.M., 2016. The transcardiac gradient of cardio-microRNAs in the failing heart. European Journal of Heart Failure 18:1000–1008.

[79] Zhou, X., Sun, F., Luo, S., Zhao, W., Yang, T., Zhang, G., et al., 2017. Let-7a is an antihypertrophic regulator in the heart via targeting calmodulin. International Journal of Biological Sciences 13:22–31.

[80] Hannafon, B.N., Carpenter, K.J., Berry, W.L., Janknecht, R., Dooley, W.C., Ding, W.Q., 2015. Exosome-mediated microRNA signaling from breast cancer cells is altered by the anti-angiogenesis agent docosahexaenoic acid (DHA). Molecular Cancer 14:133.

[81] Li, Y., Tang, X., He, Q., Yang, X., Ren, X., Wen, X., et al., 2016. Overexpression of mitochondria mediator gene TRIAP1 by miR-320b loss is associated with progression in nasopharyngeal carcinoma. PLoS Genetics 12:e1006183.

[82] Serguienko, A., Grad, I., Wennerstrom, A.B., Meza-Zepeda, L.A., Thiede, B., Stratford, E.W., et al., 2015. Metabolic reprogramming of metastatic breast cancer and melanoma by let-7a microRNA. Oncotarget 6:2451–2465.

[83] Nunez Lopez, Y.O., Victoria, B., Golusinski, P., Golusinski, W., Masternak, M.M., 2018. Characteristic miRNA expression signature and random forest survival analysis identify potential cancer-driving miRNAs in a broad range of head and neck squamous cell carcinoma subtypes. Reports of practical oncology and radiotherapy. Journal of Greatpoland Cancer Center in Poznan and Polish Society of Radiation Oncology 23:6–20.

[84] Frost, R.J.A., Olson, E.N., 2011. Control of glucose homeostasis and insulin sensitivity by the Let-7 family of microRNAs. Proceedings of the National Academy of Sciences of the United States of America 108: 21075–21080.

[85] Nunez Lopez, Y.O., Pratley, R.E., 2018. Pioglitazone alters the cargo composition of circulating exosomes in subjects with type 2 diabetes. In: American Diabetes Association's 78th Scientific Sessions. Orlando, FL: American Diabetes Association.

[86] Dahlmans, D., Houzelle, A., Andreux, P., Jorgensen, J.A., Wang, X., de Windt, L.J., et al., 2017. An unbiased silencing screen in muscle cells identifies miR-320a, miR-150, miR-196b, and miR-34c as regulators of skeletal muscle mitochondrial metabolism. Molecular Metabolism 6:1429–1442.

[87] Holman, R.R., Paul, S.K., Bethel, M.A., Matthews, D.R., Neil, H.A., 2008. 10-year follow-up of intensive glucose control in type 2 diabetes. New England Journal of Medicine 359:1577–1589.

[88] Kawata, K., Hatano, A., Yugi, K., Kubota, H., Sano, T., Fujii, M., et al., 2018. Trans-omic analysis reveals selective responses to induced and basal insulin across signaling, transcriptional, and metabolic networks. iScience 7:212–229.

[89] Daitoku, H., Sakamaki, J., Fukamizu, A., 2011. Regulation of FoxO transcription factors by acetylation and protein-protein interactions. Biochimica et Biophysica Acta 1813:1954–1960.

[90] Wang, R.H., Xu, X., Kim, H.S., Xiao, Z., Deng, C.X., 2013. SIRT1 deacetylates FOXA2 and is critical for Pdx1 transcription and beta-cell formation. International Journal of Biological Sciences 9:934–946.

[91] Yalley, A., Schill, D., Hatta, M., Johnson, N., Cirillo, L.A., 2016. Loss of interdependent binding by the FoxO1 and FoxA1/A2 forkhead transcription factors culminates in perturbation of active chromatin marks and binding of transcriptional regulators at insulin-sensitive genes. Journal of Biological Chemistry 291:8848–8861.

[92] Thomou, T., Mori, M.A., Dreyfuss, J.M., Konishi, M., Sakaguchi, M., Wolfrum, C., et al., 2017. Adipose-derived circulating miRNAs regulate gene expression in other tissues. Nature.

[93] Cansell, C., Luquet, S., 2012. Hypothalamic regulation of energy balance: a key role for DICER miRNA processing in arcuate POMC neurons. Molecular Metabolism 2:55–57.

[94] Schneeberger, M., Altirriba, J., Garcia, A., Esteban, Y., Castano, C., Garcia-Lavandeira, M., et al., 2012. Deletion of miRNA processing enzyme Dicer in POMC-expressing cells leads to pituitary dysfunction, neurodegeneration and development of obesity. Molecular Metabolism 2:74–85.

[95] Lehrke, M., Lazar, M.A., 2005. The many faces of PPARγ. Cell 123:993–999.

[96] Rosen, E.D., Sarraf, P., Troy, A.E., Bradwin, G., Moore, K., Milstone, D.S., et al., 1999. PPARγ is required for the differentiation of adipose tissue in vivo and in vitro. Molecular Cell 4:611–617.

[97] Sharma, A.M., Staels, B., 2007. Review: Peroxisome proliferator-activated receptor gamma and adipose tissue – understanding obesity-related changes in regulation of lipid and glucose metabolism. The Journal of Clinical Endocrinology and Metabolism 92:386–395.

[98] Taylor, R., Al-Mrabeh, A., Zhyzhneuskaya, S., Peters, C., Barnes, A.C., Aribisala, B.S., et al., 2018. Remission of human type 2 diabetes requires decrease in liver and pancreas fat content but is dependent upon capacity for beta cell recovery. Cell Metabolism 28:547–556 e543.

[99] Guay, C., Regazzi, R., 2013. Circulating microRNAs as novel biomarkers for diabetes mellitus. Nature Reviews Endocrinology 9:513–521.

[100] Yang, W.M., Jeong, H.J., Park, S.W., Lee, W., 2015. Obesity-induced miR-15b is linked causally to the development of insulin resistance through the repression of the insulin receptor in hepatocytes. Molecular Nutrition & Food Research 59:2303–2314.

[101] Kornfeld, J.W., Baitzel, C., Konner, A.C., Nicholls, H.T., Vogt, M.C., Herrmanns, K., et al., 2013. Obesity-induced overexpression of miR-802 impairs glucose metabolism through silencing of Hnf1b. Nature 494:111–115.

